The Geological Society of America
Special Paper 536

# *Records of late Quaternary environmental change from high-elevation lakes in the Ruby Mountains and East Humboldt Range, Nevada*

**Jeffrey S. Munroe***
**Matthew F. Bigl**
**Annika E. Silverman**
*Geology Department, Middlebury College, Middlebury, Vermont 05753, USA*

**Benjamin J.C. Laabs**
*Department of Geosciences, North Dakota State University, Fargo, North Dakota 58102, USA*

## ABSTRACT

**Sedimentary records were analyzed from three lakes in the Ruby Mountains and East Humboldt Range of northeastern Nevada. Lakes are rare in the arid Great Basin, and these represent the highest-elevation lacustrine records from this region. The three cores cover overlapping time intervals: One, from a lake located just beyond a moraine, is interpreted to represent the Last Glacial Maximum, extending back to 26 cal ka; another extends to deglaciation ca. 14 cal ka; and the third extends to deposition of the Mazama ash, ca. 7.7 cal ka. Multiproxy analysis focused on measurements of bulk density, organic matter content, C:N ratio, biogenic silica abundance, and grain-size distribution. Depth-age models were developed using optically stimulated luminescence (OSL) dating, along with accelerator mass spectrometry (AMS) $^{14}$C dating of terrestrial macrofossils (wood and conifer needles), charcoal, and pollen concentrates (for deep sediment in one lake). Collectively, the three lakes record a series of discrete intervals spanning an unusually long stretch of time. These include the local Last Glacial Maximum (26.0–18.5 cal ka), local deglaciation (18.5–13.8 cal ka), the onset of biologic productivity (13.8–11.3 cal ka), early Holocene aridity (11.3–7.8 cal ka), deposition and reworking of the Mazama ash (7.8–5.5 cal ka), a neopluvial interval (5.5–3.8 cal ka), a variable late Holocene climate (3.8–0.25 cal ka), and a latest Holocene productivity spike (250 yr B.P. to the present) that may be anthropogenic. Data from all three lakes are presented, and the collective record of climate and environmental change for the Ruby Mountains and East Humboldt Range is compared with other paleorecords from the Great Basin.**

*Corresponding author: jmunroe@middlebury.edu.

Munroe, J.S., Bigl, M.F., Silverman, A.E., and Laabs, B.J.C., 2018, Records of late Quaternary environmental change from high-elevation lakes in the Ruby Mountains and East Humboldt Range, Nevada, *in* Starratt, S.W., and Rosen, M.R., eds., From Saline to Freshwater: The Diversity of Western Lakes in Space and Time: Geological Society of America Special Paper 536, https://doi.org/10.1130/2018.2536(03). 

## INTRODUCTION

Long, continuous records of Pleistocene and Holocene environmental change are rare from the Great Basin of the southwestern United States because lakes are uncommon features in this arid landscape. Nonetheless, lakes are present in formerly glaciated ranges such as the contiguous Ruby Mountains and East Humboldt Range of northeastern Nevada. Striking alpine glacial geomorphology testifies to the former presence of cirque and valley glaciers in these mountains, which hosted the largest concentration of glacial ice between the Sierra Nevada and the Wasatch Range during the Last Glacial Maximum (Sharp, 1938). Lakes impounded by moraines and occupying depressions carved into bedrock by glacial erosion presumably formed soon after deglaciation in the Ruby Mountains and East Humboldt Range, offering the potential for long, continuous records of paleoclimate and paleoenvironmental variability.

Given the unusual abundance of lakes in the Ruby Mountains and East Humboldt Range, and the dearth of lacustrine-based paleoclimate and paleoenvironmental records for high elevations of the Great Basin, this study was designed to develop a composite lacustrine-based paleorecord for these mountains using cores from multiple lakes. Cores were retrieved from three lakes, none of which had been studied previously, and all of which were located in the headwaters of glaciated drainages on the east side of the mountains. Cores were analyzed for an array of proxies sensitive to conditions both within the lake, as well as within the surrounding watershed. Proxy measurements were converted to time series using depth-age models constructed through accelerator mass spectrometry (AMS) $^{14}C$ dating, geochemical fingerprinting of the Mazama ash, and (for one lake) optically stimulated luminescence (OSL) dating of basal sediment. Results from the three lakes were integrated as a collective record of climatic and environmental change in northeastern Nevada during and since the last glaciation. This record was then compared with previously published interpretations from elsewhere in the region.

## SETTING

The Great Basin is an extensive area of internal drainage spanning from Oregon to southern California, and from western Utah to the eastern slope of the Sierra Nevada (Fig. 1). Uplift of the Sierra Nevada in the Cenozoic cast a progressively deeper rain shadow over this region by significantly limiting delivery of moisture from the Pacific Ocean by westerly winds (Poage and Chamberlain, 2002). At the same time, profound crustal extension promoted the formation of a horst-and-graben landscape in which north-south–oriented mountain ranges were separated from one another by relatively low-lying valleys (Stewart, 1971). Maximum summit elevations are in excess of 4 km above sea level (asl) in many ranges, whereas most valley floors are at elevations of <2 km asl. As a result, the Basin and Range landscape is characterized by pronounced local gradients in elevation and moisture (Grayson, 2011).

Many of the higher mountain ranges hosted alpine glaciers during the Pleistocene, and although these glaciers were generally small (<20 km long), they produced typical alpine glacial landforms focused at higher (>2.2 km asl) elevations (Sharp, 1938, 1940; Osborn and Bevis, 2001; Wayne, 1984). Tarns are now present in some of the cirques eroded by these glaciers, and in some places, lakes are dammed behind cirque-floor moraines. The greatest concentration of glacial lakes is in the Ruby Mountains and East Humboldt Range (Fig. 1), and this project involved retrieving and analyzing sediment cores from three of them: Angel, Overland, and Soldier Lakes (Fig. 1).

Angel Lake is the northernmost of the three studied lakes (Fig. 1) and is located in a deep cirque at the head of Willow Creek (Fig. 2). The surface of the lake was raised slightly (<2 m) by a dam built in the 1930s, but most of the lake is impounded behind a recessional moraine (Munroe and Laabs, 2011). The Angel Lake area was designated as the type locality for the local Last Glacial Maximum (marine oxygen isotope stage [MIS] 2) Angel Lake glaciation in the Great Basin (Sharp, 1938). Cosmogenic surface-exposure ages for erratic boulders on the terminal moraine down valley from the lake indicate that the maximum advance of the Angel Lake glaciation occurred ca. 19 ka B.P. (Munroe and Laabs, 2011; Munroe et al., 2015) and that the moraine damming the lake was abandoned ca. 16 ka (Munroe et al., 2015). Angel Lake has a surface area of 6.4 ha and a maximum depth of 11 m and is fed by a perennial stream draining a higher cirque to the west (Table 1).

Overland Lake is the southernmost of the lakes considered in this study (Fig. 1), and it is located at the head of Overland Creek. The lake is a tarn on the floor of a deep cirque, and it does not appear to be dammed by a moraine (Fig. 2). Moraines representing the Angel Lake glaciation are found ~2 km down the valley, whereas a cirque above the lake contains talus and

TABLE 1. PROPERTIES OF LAKES AND CORES IN THE RUBY MOUNTAINS AND EAST HUMBOLDT RANGE

| Lake name | Maximum depth (m) | Mean depth (m) | Watershed area ($m^2$) | Lake area ($m^2$) | Ratio | Lake volume* ($m^3$) | Volume/ watershed (m) | Core latitude (°N) | Core longitude (°W) | Core length (cm) | Water depth (m) |
|---|---|---|---|---|---|---|---|---|---|---|---|
| Angel | 11.0 | 6.5 | 1,539,000 | 64,400 | 23.6 | 371,000 | 0.24 | 41.02590 | 115.08690 | 454 | 9.1 |
| Overland | 18.0 | 8.3 | 564,000 | 53,400 | 10.5 | 403,000 | 0.71 | 40.45958 | 115.45632 | 470 | 16.5 |
| Soldier | 3.1 | 0.8 | 248,000 | 20,900 | 11.9 | 17,000 | 0.07 | 40.73395 | 115.27402 | 415 | 3.0 |

*Calculated from interpolated bathymetry.

rockfall deposits. The lake is fed by a perennial stream and several seasonal inflows. The lake outlet has been slightly modified, making it difficult to determine whether overflow was originally perennial or seasonal. Overland Lake has a surface area of 5.3 ha and a maximum depth of 18 m (Table 1).

Soldier Lake is located roughly midway between Angel and Overland Lakes (Fig. 1). The lake is positioned on a relatively flat plateau that backs up against higher topography (Fig. 2). The lake is impounded behind a belt of moraines thought to date to the penultimate (MIS 6) glaciation, known in this region as the Lamoille glaciation after moraines on the western side of the Ruby Mountains at the mouth of Lamoille Canyon (Sharp, 1938; Wayne, 1984). Immediately upslope from Soldier Lake, there is a series of sharp-crested moraines with a fresher appearance and relatively unweathered erratic boulders that are inferred to represent the maximum extent of the Angel Lake glacial advance. Soldier Lake has a surface area of 2.1 ha and a maximum depth of 3.1 m (Table 1). The lake is fed by a few small springs, and Soldier Creek leaves the lake through an ephemeral outlet cut across the impounding moraine.

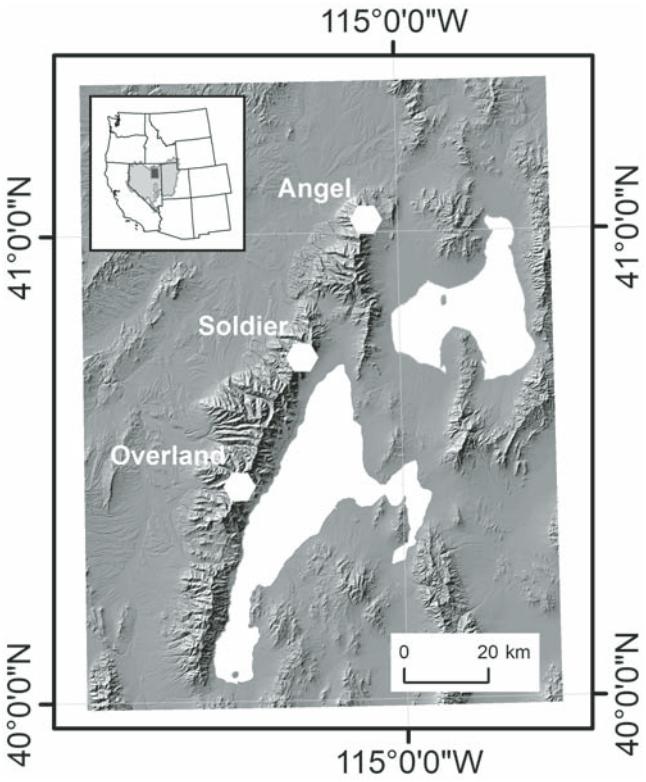


Figure 1. Shaded relief image showing the locations of the three lakes cored in this study, the Ruby Mountains and East Humboldt Range, and the former extents of pluvial Lakes Clover and Franklin (white), north and south, respectively (Munroe and Laabs, 2013a, 2013b; Mifflin and Wheat, 1979). Inset shows the location of the Great Basin (gray) in the southwestern United States and the area of the enlargement (black).

## METHODS

### Field Methods

Cores were collected from Angel, Soldier, and Overland Lakes using a combination of techniques. All three lakes were cored from a floating platform, anchored over the depocenter after completion of a bathymetric survey using a global positioning system (GPS)–enabled sonar device. Given the shallow water depth, the sedimentary record from Soldier Lake was collected entirely with a 5-cm-diameter Livingstone corer (Livingstone, 1955). For Angel Lake, the uppermost ~80 cm section, including an intact sediment-water interface, was retrieved using a Livingstone corer fitted with a clear plastic tube. Near-surface sediment (<80 cm) was collected from Overland Lake using a UWITEC Complete Corer (UWITEC, Mondsee, Austria). In both lakes, a Livingstone corer was then used to collect more-consolidated sediment between ~0.5 and 1.5 m below the sediment-water interface. Finally, a modified Reasoner-type percussion corer (Reasoner, 1993) with an ~30 kg driving weight was used to collect sediment down to the point of refusal. The percussion corer utilized a 6-m-long barrel of 7.5-cm-diameter polyvinyl chloride (PVC) pipe. Driving of the percussion corer began at the sediment-water interface, but it was not possible to retrieve the unconsolidated near-surface sediment with this technique.

Cores of near-surface sediment (Livingstone clear tube and UWITEC) were subsampled on the lakeshore at 1 cm intervals into Whirlpak bags. Deeper Livingstone drives were extruded, wrapped in plastic film and aluminum foil, and transported in collapsible core boxes. Percussion cores were cut to ~0.8 m lengths with a hacksaw, capped, and shipped in hard-sided boxes. All core sections and subsamples were stored at 4 °C until processing.

### Laboratory Methods

The Livingstone cores from Soldier Lake were opened in the Geography Department at The Ohio State University, and subsamples (at 1-cm intervals) were delivered to Middlebury College, Middlebury, Vermont. Surface, Livingstone, and percussion cores from Angel and Overland Lakes were shipped directly to Middlebury College. Before opening, percussion core sections were X-rayed and run through a Bartington magnetic susceptibility (MS) meter connected to a 12-cm-diameter loop for measurement of volume magnetic susceptibility at 1 cm intervals. The MS meter was re-zeroed every 50 cm, and a drift correction was applied to all measurements. MS measurements were not made on near-surface sediments collected with the UWITEC (Overland Lake) or Livingstone clear tube (Angel Lake) that were subsampled in the field. Percussion core sections were opened by cutting the PVC lengthwise with a circular saw and pulling a thin wire from top to bottom. Livingstone core sections were unwrapped and split with a knife. Freshly opened cores were photographed, and visual stratigraphy was recorded. Half of each core section

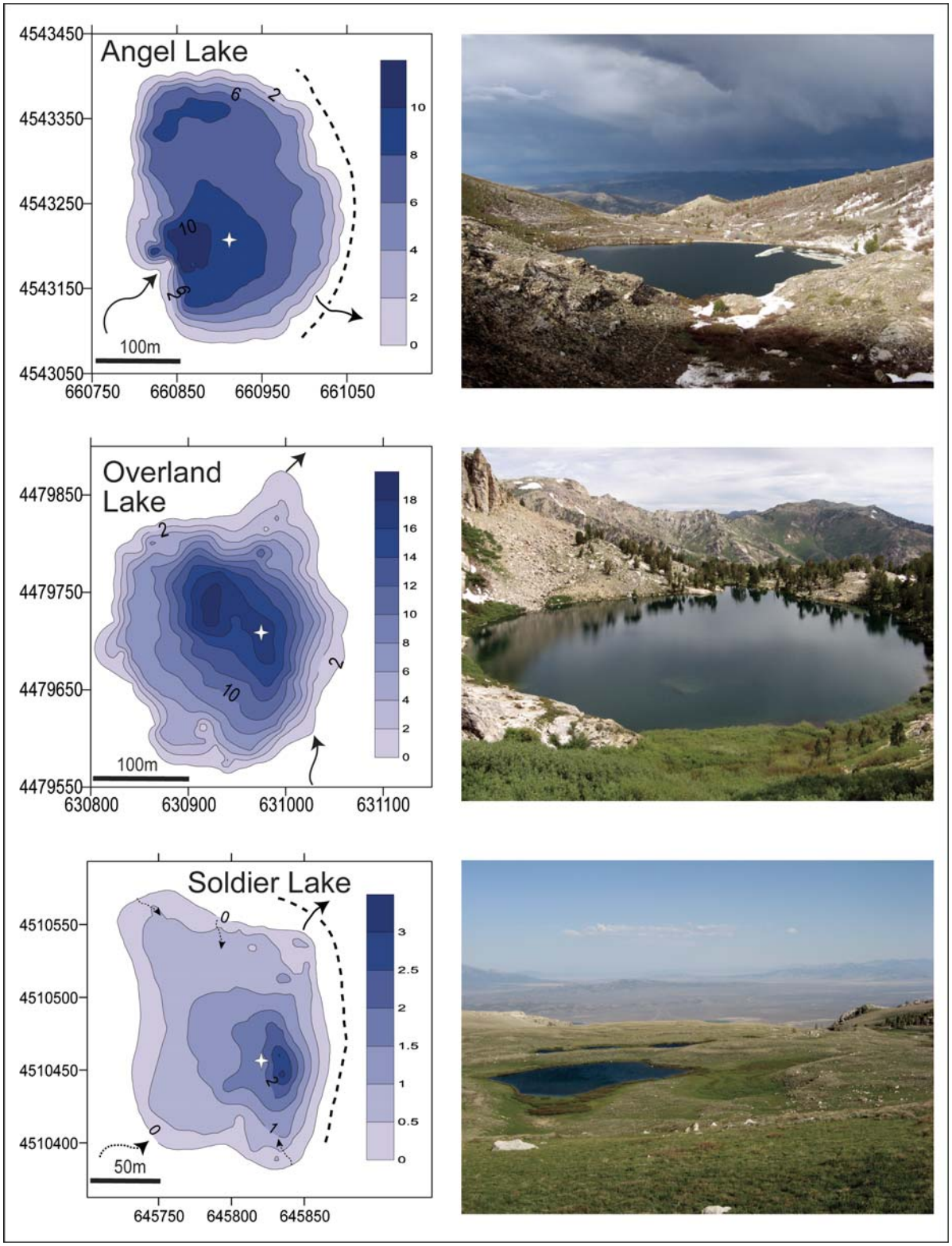


Figure 2. Bathymetric maps for the cored lakes with Universal Transverse Mercator (UTM) coordinates given within Zone 11N. Depths are in meters, and the white star marks the coring location. Perennial inlets and outlets to Angel and Overland Lakes (solid arrows), and the ephemeral inlet and outlet to Solder Lake (dashed arrows) are shown, along with submerged channels visible on the floor of Solder Lake (thin dotted arrows). Moraines impounding Angel and Soldier Lakes are denoted by thick dashed lines. Right column presents photographs of each lake: Angel Lake view is to the east (photo by J. Munroe on 15 June 2010, taken from a point 300 m west of Angel Lake), Overland Lake view is to the north (photo by J. Munroe on 11 July 2009, taken from a point 100 m south of Overland Lake), and Soldier Lake view is to the southeast (photo by J. Munroe on 26 June 2012, taken from a point 200 m northwest of Soldier Lake).

was wrapped in 46 gauge Saran 8 and heat-sealed inside a shrink-wrap sleeve before being archived at 4 °C. The other half of each section was subsampled at 1 cm resolution in quadruplicate.

The entire collection of subsamples from all three lakes was analyzed for a consistent set of physical and chemical properties, most at 1 cm intervals. Water content and loss-on-ignition at 550 °C were determined with a Leco TGA 701 thermogravimetric analyzer. Loss-on-ignition is considered a proxy for organic matter (OM) content (Dean, 1974). Water content, which reflects bulk density (Menounos, 1997), was determined from the mass lost during heating to 105 °C under a full nitrogen atmosphere for 4 h. Abundance of OM was determined from mass lost from the dried sample over 3 h at 550 °C under ambient atmosphere.

Biogenic silica (bSi) content was determined for freeze-dried samples (1 cm intervals in Overland Lake, and 2 cm intervals in Angel and Soldier Lakes) by sequential extraction while leaching in 0.1 *M* NaOH for 5 h at 85 °C (DeMaster, 1981). Dissolved Si content was determined for each aliquot by spectrophotometry at 812 nm after addition of reagents for a molybdate blue reaction (Strickland and Parsons, 1965). The bSi (in wt%) was calculated from the *y* intercept of a linear function fit to the results for extractions for hours 2 through 5. Analysis of replicates indicated that this method has a reproducibility of 10%. The abundance of bSi was added to the OM value determined through loss-on-ignition and subtracted from 100 to yield an estimate for the abundance of terrestrial mineral material in the sediment (% clastic).

The abundance of carbon and nitrogen in each sample was determined with a Thermo Flash 2000 elemental analyzer calibrated with aspartic acid. No detectable change was observed in measured carbon values after a subset of samples was acidified and reanalyzed, and so all carbon in these samples was inferred to be organic.

Wet bulk density (BD) was determined from the wet volume and freeze-dried mass of samples from Overland Lake using a Quantachrome pentapycnometer. A fourth-order polynomial describing the relationship between water content and BD ($R^2$ = 0.9032) was then used to estimate values of BD for samples from Angel and Soldier Lakes from their measured water contents. The possible limitations of this indirect approach were considered acceptable because interpretation was focused on BD trends, rather than absolute values. Furthermore, measurements of wet BD were not possible on the Soldier Lake core, which had dried before analysis.

Grain size (GS) distribution was determined with laser scattering in a Horiba LA-950 after treatment with 35% $H_2O_2$ (three additions of 10 mL over 7–10 d) to remove OM and 0.1 *M* NaOH (1 h, 85 °C) to remove biogenic silica. This instrument has an effective range from 10 nm to 3 mm. Sodium hexametaphosphate (3%) was used as a dispersant.

## Interpretive Framework

Each of the proxies measured in this study is equivocal in isolation, but together they can be used to infer the type of environmental changes they represent. For instance, proxies such as MS and GS represent the type and amount of terrestrial clastic sediment delivered by inflowing streams. Both Angel and Overland Lakes are fed by perennial streams with considerable discharge. Both are located in steep-walled basins, and both overflow freely across wide sills (in its natural state, Angel Lake would have overflowed, although outflow is now controlled by the dam and associated spillway). Thus, during times of increased precipitation, both of these lakes would flush more regularly, but their water levels would not have risen appreciably, and their areas would have remained more or less constant. In contrast, Soldier Lake sits in a gently sloping basin, lacks an integrated inflow, and drains through a narrow boulder-armored notch cut across a moraine. Thus, increases in precipitation would likely drive Soldier Lake to a greatly expanded lake area. Because the bedrock upslope from each lake contains Fe-bearing minerals, inwashing of detrital sediment would increase MS and the average GS of the sediment. Inwashing to Angel and Overland Lakes would increase with enhanced precipitation; given its position, small watershed, and lack of inflowing streams, inwashing to Soldier Lake would increase with glacial advance.

The C:N ratio provides information about the composition of OM accumulating in the lake, with higher values indicative of terrestrial (woody) vegetation and lower values representing algal material (Meyers and Ishiwatari, 1993). Increases in biogenic silica and OM content, particularly when combined with low C:N values indicative of aquatic OM, are interpreted as signals of elevated in-lake productivity. Given that these lakes are located at high elevations in environments dominated for much of the year by snow and ice, increased aquatic productivity is considered to be a sign of increased summer temperatures, leading to warmer water temperatures and/or an increase in the duration of the ice-free period (McKay et al., 2008).

Sediment bulk density and % clastic integrate the abundance of relatively low-density OM (from within and around the lake) and relatively high-density mineral material (primarily from the watershed). As a result, these proxies incorporate both sediment inwashing and organic productivity.

## Geochronology

Depth-age models were derived for these cores using radiocarbon dating, tephrachronology, and OSL (for Angel Lake). In total, 16 AMS $^{14}C$ ages were determined at the National Ocean Sciences Acceleratory Mass Spectrometry facility on samples of wood, conifer needles, charcoal, and concentrated pollen (Table 2). Depth-age models were developed using the smoothed-spline function in CLAM (Blaauw, 2010), which utilizes the Intcal13 calibration curve (Reimer et al., 2013). Calibrated radiocarbon ages are designated as "cal" ka. Samples of a prominent ash layer encountered at a depth of ~330 cm in the Overland Lake core, and at 195 cm in the core from Soldier Lake, were submitted to the U.S. Geological Survey (USGS) Tephrochronology Laboratory for geochemical fingerprinting. These samples were

TABLE 2. RADIOCARBON AGES FOR CORES FROM LAKES IN THE RUBY MOUNTAINS AND EAST HUMBOLDT RANGE

| Lab number | Lake | Sample | Description | Strat depth* (m) | No ash depth (m) | $\delta^{13}C$ (‰) | F modern† | Fm error§ | $^{14}C$ age (yr B.P.) | Age error (+/-) | 2-sig ranges (*Prob*) | Median cal yr B.P. |
|---|---|---|---|---|---|---|---|---|---|---|---|---|
| OS-66112 | Angel | AL-2_5 | Wood | 43.5 | 43.5 | –26.48 | 0.9295 | 0.0035 | 585 | 30 | 535–570 (*0.307*), **581–651 (*0.693*)** | 600 |
| OS-67027 | Angel | AL-2P 100 | Wood | 138.5 | 138.5 | –27.31 | 0.765 | 0.0025 | 2150 | 25 | **2048–2164 (*0.670*),** 2166–2180 (*0.024*), 2241–2303 (*0.306*) | 2140 |
| OS-67028 | Angel | AL-2P 186 | Wood | 224.5 | 224.5 | –22.48 | 0.5766 | 0.0023 | 4420 | 30 | **4870–5062 (*0.875*),** 5113–5118 (*0.005*), 5221–5239 (*0.019*), 5241–5268 (*0.030*) | 5000 |
| OS-71527 | Angel | AL2P 212 | Wood | 250.5 | 250.5 | –23.98 | 0.6167 | 0.0018 | 3880 | 25 | **4240–4412 (*1.000*)** | 4330 |
| OS-67029 | Angel | AL-2P 282 | Wood | 320.5 | 320.5 | –25.85 | 0.5576 | 0.0023 | 4690 | 30 | **5320–5424 (*0.664*),** 5433–5476 (*0.233*), 5541–5576 (*0.103*) | 5400 |
| OS-67055 | Angel | AL-2P 393 | Wood | 431.5 | 431.5 | –25.32 | 0.4806 | 0.0023 | 5890 | 40 | 6575–6576 (*0.001*), **6633–6797 (*0.991*),** 6819–6830 (*0.008*) | 6710 |
| OS-78273 | Overland | 09-01d_9 | Needles | 48 | 48 | –22.99 | 0.8514 | 0.0028 | 1290 | 25 | 1181–1214 (*0.360*), **1221–1284 (*0.640*)** | 1240 |
| OS-78274 | Overland | 09-01d_55 | Wood | 94 | 94 | –23.58 | 0.7552 | 0.0025 | 2250 | 25 | **2158–2260 (*0.660*),** 2299–2341 (*0.340*) | 2230 |
| OS-78275 | Overland | 09-01d_131 | Wood | 170 | 170 | –22.68 | 0.6857 | 0.0026 | 3030 | 30 | 3084–3087 (*0.002*), 3145–3152 (*0.009*), **3155–3277 (*0.712*),** 3281–3344 (*0.277*) | 3230 |
| OS-78276 | Overland | 09-01d_247 | Wood | 286 | 286 | –23.05 | 0.5042 | 0.002 | 5500 | 30 | 6217–6238 (*0.065*), **6272–6324 (*0.797*),** 6328–6350 (*0.045*), 6367–6395 (*0.094*) | 6300 |
| OS-78277 | Overland | 09-01d_333 | Wood | 372 | 355 | –25.77 | 0.3604 | 0.0016 | 8200 | 35 | **9030–9269 (*1.000*)** | 9160 |
| OS-78278 | Overland | 09-01d_414 | Wood | 453 | 436 | –28.19 | 0.2323 | 0.0014 | 11700 | 45 | **13,431–13,599 (*1.000*)** | 13,520 |
| OS-92166 | Soldier | GBSLD11_108cm | Wood | 108 | 108 | –27.64 | 0.8233 | 0.0028 | 1560 | 25 | **1396–1526 (*1.000*)** | 1470 |
| OS-92167 | Soldier | GBSLD11_216cm | Charcoal | 216 | 212 | –25.46 | 0.3399 | 0.0017 | 8670 | 40 | **9540–9704 (*0.995*),** 9723–9729 (*0.005*) | 9610 |
| OS-101202 | Soldier | Soldier-300 | Pollen | 300 | 296 | –21.72 | 0.2151 | 0.0015 | 12350 | 55 | **14,105–14,718 (*1.000*)** | 14,360 |
| OS-101153 | Soldier | Soldier-400 | Pollen | 400 | 396 | –20.2 | 0.0766 | 0.0008 | 20600 | 85 | **24,474–25,151 (*1.000*)** | 24,810 |

*Strat depth—stratigraphic depth.
†F modern—fraction modern C.
§Fm error—fraction modern C error.

identified as Mazama ash, and an age of 7627 ± 150 yr B.P. for the Mazama ash was used in the depth-age models (Zdanowicz et al., 1999). A sample from the base of the Angel Lake core was submitted to the Luminescence Laboratory at Utah State University. This sample yielded a single aliquot regenerative (SAR)–OSL age of 7940 ± 900 yr B.P. Given this result, tephra encountered at the base of this core was also assumed to be Mazama ash.

## RESULTS

### Angel Lake

Coring efforts at Angel Lake generated a complete stratigraphy down to the Mazama ash layer. The 74-cm-long surface core preserved an intact sediment-water interface with live chironomids. Sediment below the flocculent surface layer (1 cm thick) was primarily massive gyttja, with a Munsell color of 2.5Y 2.5/1 (black). The surface core overlapped stratigraphically with the percussion core, which penetrated to a depth of ~450 cm. Visual inspection, supplemented by X-radiography, revealed that much of the percussion core features sub-centimeter-scale laminations defined by contrasts in GS distribution, primarily sand content (Fig. 3). The upper ~80 cm section of the percussion core is generally massive and vesicular; however, alternations in lightness/darkness, concentrations of large sand grains, flecks of white mica, and small pebbles become increasingly common with depth (Fig. 3). Sediment generally has Munsell colors of 2.5Y 2.5/1 (black) to 5Y 2.5/1 (black). Minimal down-warping of sedimentary layers along the edges of the core tube indicates that disturbance during coring was limited.

Six samples of terrestrial OM were radiocarbon dated from the Angel Lake percussion core, yielding calibrated ages ranging from ca. 6.7 to ca. 0.6 cal ka (Table 2). One age, 4420 ± 30 yr B.P. at a true depth of 225 cm, was stratigraphically reversed (Table 2). The remaining five ages were combined with the SAR-OSL age of 7940 ± 900 B.P. for the core bottom, the 7627 ± 150 yr B.P. age for the Mazama ash, and an estimate of A.D. 2007 for the surface to construct a smoothed spline depth-age model in CLAM (Fig. 3). The model is nearly linear, and the width of the 95% error envelope is minimal (<200 yr) through most of the record, although it widens to a maximum of 550 yr approaching the core base (Fig. 3). The overall average sedimentation rate through the core is 6.15 cm/century. The stratigraphically reversed age was obtained on a wood fragment from a notably coarse, poorly sorted layer that likely represents a mass-wasting event that transported dead wood from the watershed into the lake.

When compared with the other two lakes, the physical proxies measured in the Angel Lake core tend to have intermediate values (Table 3). Mean values of OM, BD, bSi, % clastic, and MS are all between average values in Overland and Soldier Lakes.

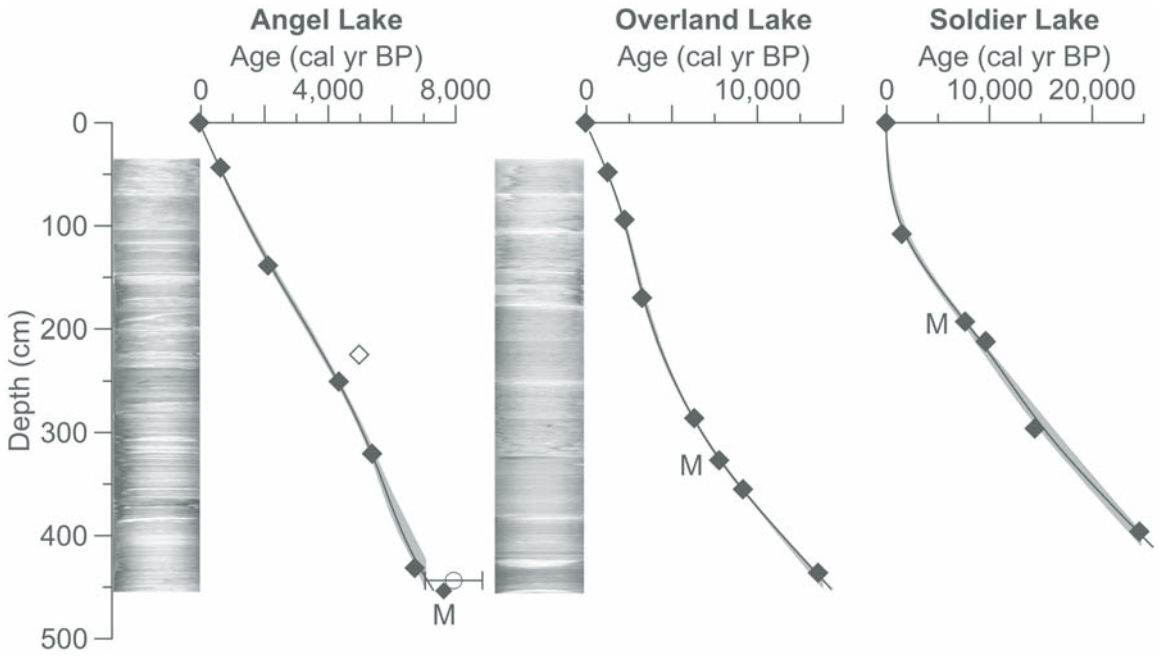


Figure 3. Depth-age models derived for Angel, Overland, and Soldier Lakes determined using CLAM (Blaauw, 2010). Black diamonds mark the median age for each calibrated $^{14}C$ date. The open diamond denotes a date that was ignored in constructing the depth-age model for Angel Lake. "M" marks the Mazama ash (Zdanowicz et al., 1999). The open circle with error bars represents the optically stimulated luminescence (OSL) age from the base of the Angel Lake core. Gray shading illustrates the error range of the age model at different depths; in many places, this narrow range is obscured by the line denoting the age model itself. X-radiographs of the Angel and Overland Lake cores are shown along the *y* axis (after removal of the Mazama ash layer); the core from Soldier Lake was not X-rayed.

TABLE 3. SUMMARY STATISTICS FOR LAKE SEDIMENT CORES FROM THE RUBY MOUNTAINS AND EAST HUMBOLDT RANGE

| | | Angel Lake | Overland Lake | Soldier Lake |
|---|---|---|---|---|
| Organic matter (%) | Mean | 13.1 | 12.7 | 14.1 |
| | Median | 12.8 | 12.9 | 14.8 |
| | St. dev. | 2.7 | 2.7 | 10.3 |
| | Range | 4.8–20.0 | 4.2–26.4 | 1.6–54.4 |
| | Number | 454 | 452 | 410 |
| Bulk density (g/cm$^3$) | Mean | 0.66 | 0.41 | 0.87 |
| | Median | 0.67 | 0.40 | 0.60 |
| | St. dev. | 0.21 | 0.13 | 0.61 |
| | Range | 0.21–1.41 | 0.02–1.30 | 0.02–1.75 |
| | Number | 454 | 452 | 406 |
| Biogenic silica, bSi (%) | Mean | 5.3 | 20.0 | 2.0 |
| | Median | 5.3 | 20.8 | 1.2 |
| | St. dev. | 1.6 | 4.6 | 1.7 |
| | Range | 0.0–9.9 | 2.1–30.4 | 0.0–8.3 |
| | Number | 247 | 227 | 206 |
| Clastic sediment (%) | Mean | 80.4 | 67.3 | 84.0 |
| | Median | 80.4 | 66.5 | 84.0 |
| | St. dev. | 3.7 | 6.6 | 11.7 |
| | Range | 72.3–92.7 | 48.5–93.6 | 37.3–98.0 |
| | Number | 247 | 227 | 206 |
| C:N | Mean | 11.4 | 11.1 | 9.7 |
| | Median | 11.3 | 11.1 | 12.2 |
| | St. dev. | 1.0 | 0.8 | 4.7 |
| | Range | 7.8–15.5 | 6.9–13.6 | 1.9–16.1 |
| | Number | 247 | 452 | 406 |
| Magnetic susceptibility, MS ($\times 10^{-5}$ SI units) | Mean | 6.3 | 9.5 | 17.7 |
| | Median | 6.0 | 9.3 | 6.5 |
| | St. dev. | 2.8 | 3.1 | 21.0 |
| | Range | 2.0–14.0 | 4.2–17.9 | 0–96.2 |
| | Number | 415 | 353 | 335 |
| Median grain size (μm) | Mean | 37.1 | 11.2 | 17.1 |
| | Median | 23.5 | 10.8 | 16.0 |
| | St. dev. | 33.4 | 2.7 | 9.6 |
| | Range | 6.4–192.0 | 5.7–32.2 | 5.0–96.6 |
| | Number | 454 | 452 | 410 |
| Accumulation rate (cm/century) | Mean | 6.15 | 3.14 | 1.58 |

Values of C:N in Angel Lake average slightly higher than in the other lakes, although this likely reflects the relative shortness of the record, which lacks sediment that accumulated before the surrounding watershed was vegetated. The most-striking difference about the Angel Lake record is the very high average for median GS (37 μm), which is almost that of Soldier Lake, the next coarsest (Table 3).

The proxies measured in Angel Lake also exhibit considerable fine-scale variability superimposed on long-term trends. BD, MS, and % clastic all decrease over time (Fig. 4). In contrast, OM increases upward through the core. Values of C:N oscillate around 12 for most of the record, but they drop dramatically in the most recent centuries to ~8. Median GS is highly variable, with fluctuations driven primarily by abrupt spikes in the abundance of sand. Maximum values of median GS range up to 192 μm, the highest values obtained in these three lakes. To further investigate the timing of these GS spikes, which are unique to the Angel Lake record, a 1000 yr running average was calculated for the median GS time series, and increases in median GS rising above this baseline were identified (Fig. 4). Temporal clustering of the coarse layers identified through this approach was assessed by calculating the number of coarse layers per century (Fig. 4). Values were highest in the middle Holocene, generally low from 4.0 to 1.5 cal ka, and rose again ca. 1.0 cal ka (Fig. 4).

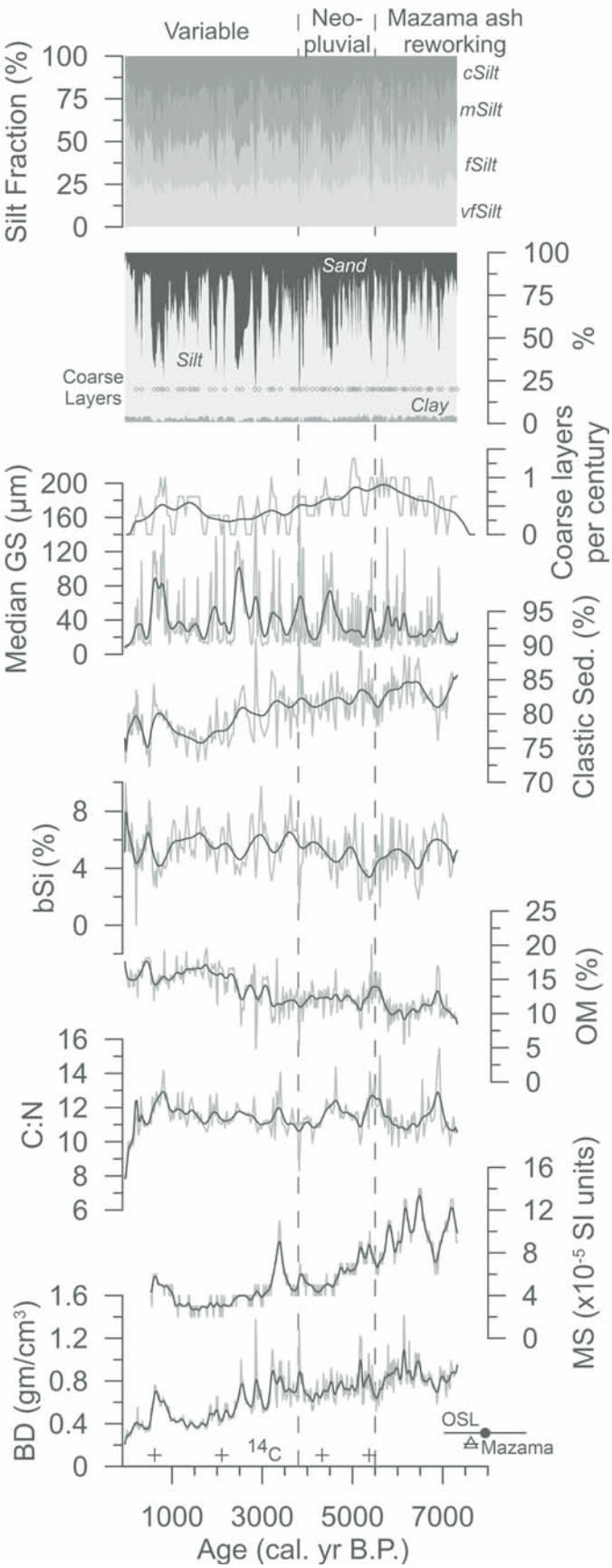


**Overland Lake**

The overlapping surface and percussion cores from Overland Lake produced a record extending from the surface down through the postglacial section (Fig. 3). The surface core contained an intact sediment-water interface and reached a depth of 69 cm. The percussion core featured diffuse centimeter-scale banding defined by subtle lightness/darkness alternations within an overall Munsell color of 2.5Y 2.5/1 (black). Gas bubbles were present throughout, but they were not as abundant as in the Angel Lake core. The visually striking Mazama ash layer spanned 18 cm, between a stratigraphic depth of 327 cm to 345 cm. The lowest 8 cm portion of this section was nearly pure tephra, with a mean grain size of 31 µm and up to 25% sand (>63 µm). The upper 10 cm portion of this section was slightly darker and finer, with a mean grain size of 23 µm and generally <10% sand. Below the Mazama ash, the layering in the sediment became more pronounced, with a general shift in overall Munsell color toward a lighter color, 5Y 4/1 (dark gray). A large cobble of pegmatite (~7 × 7 × 7 cm) embedded in coarser sediment was encountered at a depth of 423 cm, with another smaller cobble oriented parallel to bedding at a depth of 450 cm. Layers of abundant daphnia ephippia were also noted, with increasing frequency in the deepest 70 cm of the core.

In total, six radiocarbon ages, five on wood fragments and another on conifer needles, were obtained for the Overland Lake core. All of these were in stratigraphic order, with calibrated ages ranging from 13.5 to ca. 1.25 cal ka (Table 2). Together with an age of 7627 ± 150 yr B.P. for the Mazama ash (the 18 cm thickness of which was removed from the stratigraphy), and an age of A.D. 2009 for the sediment-water interface, a smoothed spline depth-age model was generated using CLAM (Fig. 3). The deepest $^{14}C$ age of 13.5 cal ka was determined for a small twig collected from just 15 cm above the core base, minimizing the extrapolation required to estimate the basal age. Error ranges (95% confidence interval) for the depth-age model were generally <200 yr, except in the lowest 70 cm, where they increased to a maximum of 600 yr. The overall average sedimentation rate is 3.14 cm/century.

In comparison to the other lakes, values of OM, BD, % clastic, C:N, and median GS are generally low in Overland Lake (Table 3), reflecting its large size, greater depth, and (possibly) its higher elevation (Table 1). One striking contrast is the extremely high average bSi value for Overland Lake (20%), which is 4× the

Figure 4. Time series of proxies measured in the Angel Lake core: bulk density (BD), magnetic susceptibility (MS, not measured in near-surface sediment), carbon:nitrogen ratio (C:N), organic matter (OM), biogenic silica (bSi), percent clastic sediment, median grain size (GS), sand/silt/clay abundance (%), and silt fraction (c—coarse; m—medium; f—fine; vf—very fine). Coarse layers were identified objectively as peaks in median grain size rising above a 1000 yr running average. Age control is noted along the bottom axis. OSL—optically stimulated luminescence.

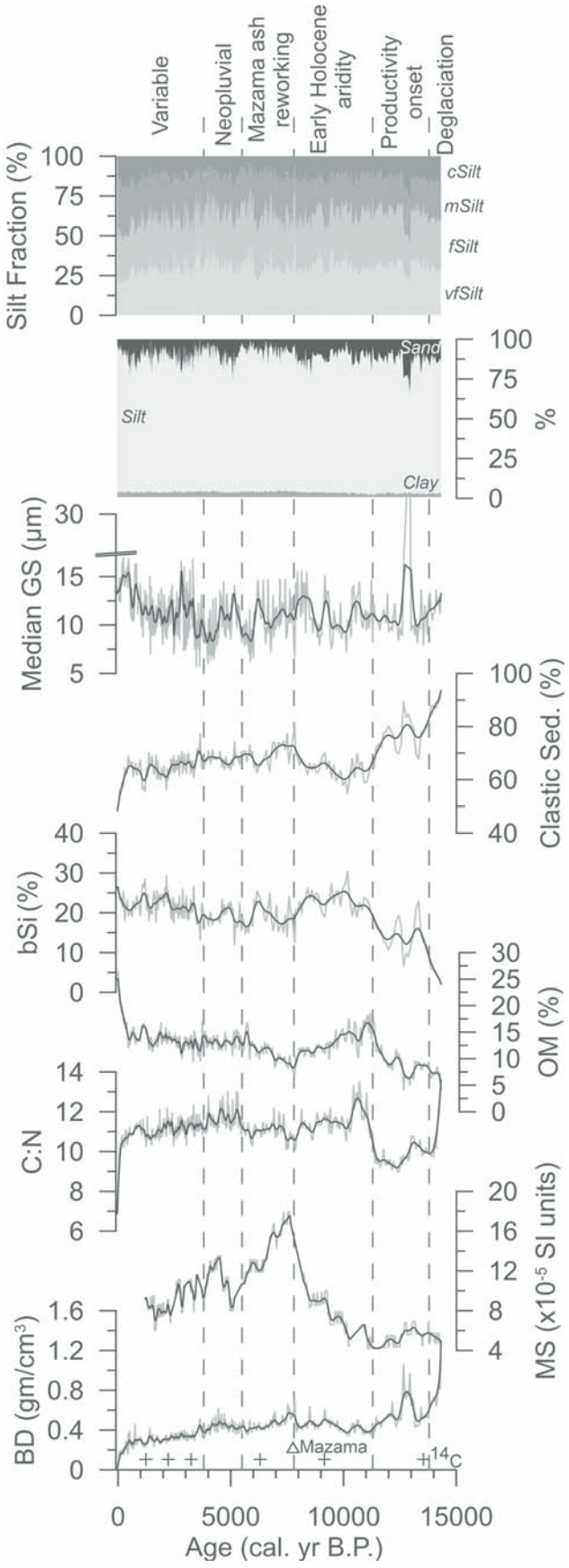


value in Angel Lake and 10× that in Soldier Lake. The reason for this difference is not clear, but it may relate to the nutrient status of the Overland Lake watershed.

Values of physical proxies in the Overland Lake core exhibit long-term trends (Fig. 5). BD and % clastic decrease upward through the core, whereas OM increases. OM values rise to a maximum value for this lake, and the C:N ratio falls to a minimum, in the most recent part of the core. MS spikes after deposition of the Mazama ash and decreases as ash reworking tapers off. Values of C:N are relatively constant around 11 after 11 cal ka, but they are <10 in the latest Pleistocene section. Median GS averages ~10 μm, was lowest around 4 cal ka, and rose to a sustained high over the past 1000 yr. High-frequency variability in sand content is superimposed on millennial-scale intervals of generally elevated sand content, spaced roughly 2 k.y. apart.

**Soldier Lake**

The sedimentary record from Soldier Lake was retrieved entirely with Livingstone coring equipment, reaching a depth of 416 cm below the sediment-water interface. The resulting 5-cm-diameter, foil-wrapped core sections were not X-rayed; however, during visual inspection, layers of coarse sand and fine gravel, some containing fragments of quartz up to 1.5 cm in diameter, were noted, particularly between depths 150 cm and 250 cm. The Mazama ash spanned from 189 to 198 cm, with the lowest 4 cm representing primary air-fall tephra. The mean GS of this material (33 μm) is nearly identical to the Mazama ash in Overland Lake. The 5 cm section of reworked tephra overlying the primary Mazama ash is finer, with a mean GS of 26 μm. Deeper in the core, below a depth of 285 cm, the sediment featured prominent partings along thin layers of fine sand. Charcoal was also noted throughout, both as macroscopic fragments and dark layers enriched in fine organic material.

Age control for the Solider Lake core is provided by four $^{14}$C ages (Table 2). The upper two are from wood and charcoal, whereas a paucity of OM in the lower half of the core necessitated the dating of pollen concentrated by centrifugation. The depth-age model was developed in CLAM using a smoothed spline fit to the four $^{14}$C ages, the sediment-water interface (A.D. 2009) and the Mazama ash, after removing the 4 cm of primary air-fall tephra from the stratigraphy (Fig. 3). The deepest $^{14}$C age was determined for sediment 15 cm above the core base, minimizing the extrapolation involved in estimating a basal age of ca. 26.0 cal ka (Table 2). The resulting model has the slowest mean sedimentation rate of the three lakes, 1.58 cm/century. In

Figure 5. Time series of proxies measured in the Overland Lake core: bulk density (BD), magnetic susceptibility (MS, not measured in near-surface sediment), carbon:nitrogen ratio (C:N), organic matter (OM), biogenic silica (bSi), percent clastic sediment, median grain size (GS), sand/silt/clay abundance, and silt fraction (c—coarse; m—medium; f—fine; vf—very fine). Age control is noted along the bottom axis.

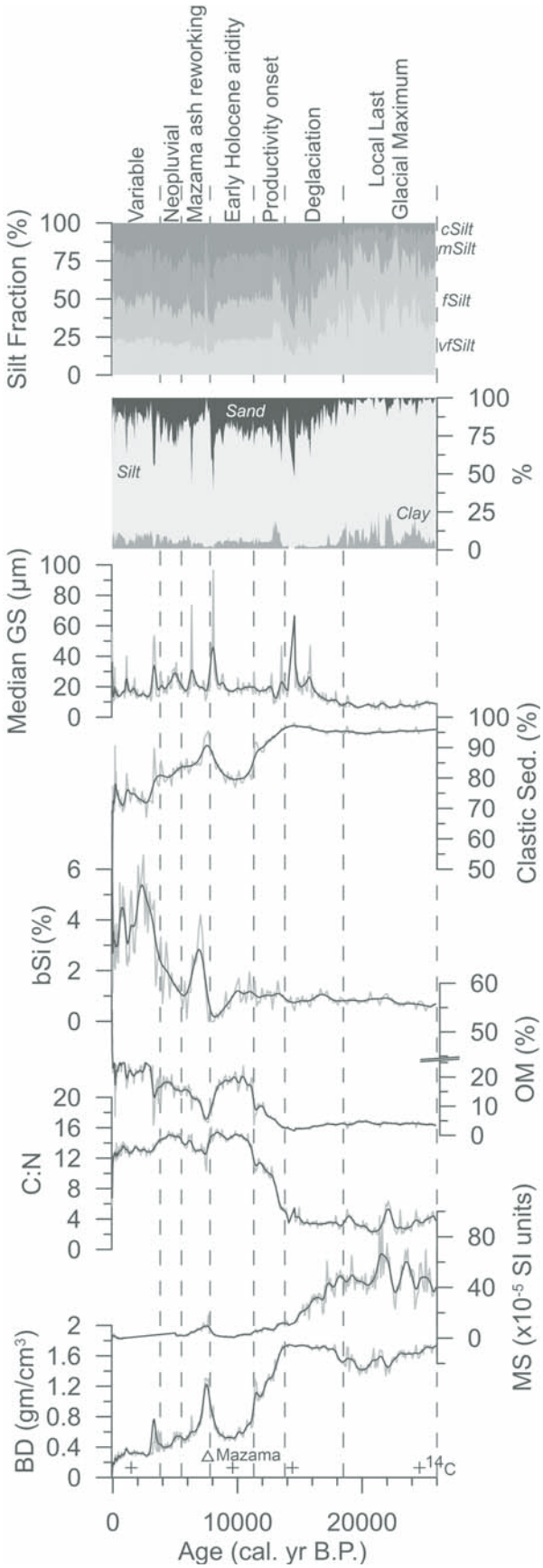


Figure 6. Time series of proxies measured in the Soldier Lake core: bulk density (BD), magnetic susceptibility (MS), carbon:nitrogen ratio (C:N), organic matter (OM), biogenic silica (bSi), percent clastic sediment, median grain size (GS), sand/silt/clay abundance, and silt fraction (c—coarse; m—medium; f—fine; vf—very fine). Age control is noted along the bottom axis.

the upper half of the core, the 95% confidence interval on the age estimates is 600 yr or less. However, in the deepest meter, the error range increases to ~1400 yr (Fig. 3).

Many proxies measured in the Soldier Lake core have high average values (Fig. 6). For instance, OM, BD, % clastic, and MS are higher in Soldier Lake than in the other two lakes (Table 3). In contrast, average values of bSi and C:N are very low (Fig. 7). Physical proxies in the Soldier Lake core also exhibit dramatically different values in the first half of the record relative to the second half (Fig. 6). Values of BD, MS, and % clastic are high in the older section and fall after 14 cal ka. In contrast, values of OM, C:N, bSi, and median GS are low and steady during the older interval and then rise markedly. Clay and very fine silt are abundant in the older sediment. Clay abundance drops to near zero between ca. 18 and 14 cal ka, while sand increases to ~25% and is constant at that level through the early Holocene.

## DISCUSSION

### Synthesis of Lake Records and Interpretation of Proxies

The three lake records considered in this study represent notably different time periods (Angel: 7700 yr, Overland: 14,000 yr, Soldier: 26,000 yr) with differing resolutions (Table 3). However, when considered collectively, they provide a unique perspective on environmental change at high elevations in the Ruby Mountains and East Humboldt Range during the local Last Glacial Maximum, the last glacial-interglacial transition, and the Holocene. To organize discussion about the sequence of environmental changes in this region during the time period represented by the cores, the records have been divided into subjectively determined zones within which the majority of measured proxies shift in consistent, interpretable directions. In this discussion, these zones are delineated, proxy patterns are described and interpreted, and correspondence with other regional paleoenvironmental records is assessed.

#### *Local Last Glacial Maximum (26.0–18.5 cal ka)*

The local Last Glacial Maximum is recorded by the core from Soldier Lake, which was positioned just outside of the terminal moraine constructed by the Soldier Creek glacier during the Angel Lake glaciation (Sharp, 1938). Sediment accumulating in the lake during the local Last Glacial Maximum had high and steady values of BD (~1.6 g/cm$^3$) and % clastic (~95%), and high and variable MS (~50 × 10$^{-5}$ SI units). The abundance of clay and very fine silt together totaled ~45% of the total GS distribution,

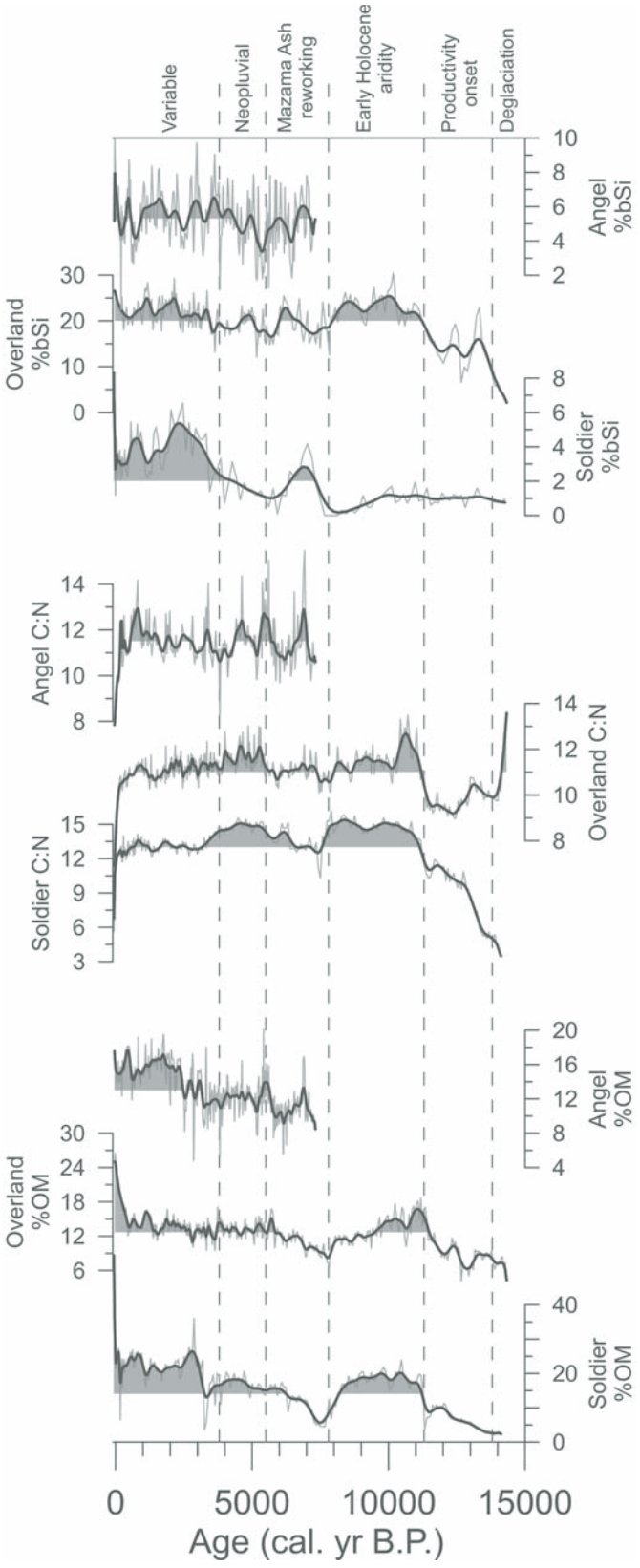


Figure 7. Comparison of organic matter (OM), carbon-nitrogen ratio (C:N), and biogenic silica (bSi) in all three lakes over the past ~14,000 yr.

much higher than at any other time during the record. In contrast, values of C:N (~4), OM (~4%), bSi (~1%), and median GS (~8 μm) were very low.

Collectively, these properties indicate that sediment accumulating in Soldier Lake during the local Last Glacial Maximum was primarily inorganic glacial rock flour, which is consistent with the location of the lake outside of the Angel Lake glacial limit. The apparent age of the rock-flour–dominated sedimentation in Soldier Lake is contemporaneous with the known timing of the global Last Glacial Maximum (LGM), which spanned the interval ca. 26–19 ka B.P. (Clark et al., 2009). Regionally, cosmogenic surface-exposure dates on moraine boulders (Phillips et al., 2009; Rood et al., 2011; Phillips, 2016), and rock flour records from Owens Lake (Bischoff and Cummins, 2001) reveal that the Tioga glaciation in the Sierra Nevada peaked at this time (Fig. 8D). Similarly, valley glaciers in the Wasatch and Uinta Mountains at the eastern border of the Great Basin (Laabs et al., 2011; Laabs et al., 2009; Munroe et al., 2006), and elsewhere in the Ruby Mountains and East Humboldt Range (Munroe et al., 2015; Laabs et al., 2013), occupied extended positions at this time.

Glacial conditions at Soldier Lake at this time are consistent with records of increased effective moisture elsewhere in the Great Basin. For instance, along the east side of the Ruby Mountains and East Humboldt Range (Fig. 1), radiocarbon dating of gastropod shells indicates that Lake Franklin inundated 43% of its ultimate highstand area beginning ca. 22 cal ka, increasing to ~60% by 20 cal ka (Munroe and Laabs, 2013a). Similarly, Lake Clover was at its highstand ca. 19 cal ka (Munroe and Laabs, 2013b), and Lake Bonneville was transgressing toward its overflow point, which it reached ca. 18 cal ka (Oviatt, 2015). Farther afield, speleothem records from southern Arizona and New Mexico (Wagner et al., 2010; Asmerom et al., 2010) also indicate wetter conditions during the early part of the local Last Glacial Maximum (Figs. 8Q and 8P), persisting to ca. 16,000 yr B.P. at Cave of the Bells, Arizona.

Overall, it appears that Soldier Lake existed as a small water body during the local Last Glacial Maximum, possibly ice covered for much of the year, just outside the terminal moraine of the Angel Lake glaciation. Changes in the abundances of fine and very fine silt during this interval (Fig. 6) may reflect short-lived advances and retreats of the nearby glacier, impacting the delivery of rock flour to the lake. Very fine silt, in particular, makes up more than 50% of the GS distribution (by volume) during these peaks, indicating that rock flour was dominating the clastic sediment load. Given the existing age model, peaks in fine and very fine silt occurred at 24.2, 22.7, 21.2, and 19.8 cal ka, suggesting a quasi-regular ~1400 yr spacing. Previous reports have noted complex behavior of alpine glaciers during the LGM, including studies of rock flour deposited in Owens Lake at the western edge of the Great Basin (Bischoff and Cummins, 2001). Furthermore, the very fine silt peak at 24.2 cal ka, which was followed by an interval of consistently high very fine silt abundance until 23.2 cal ka, may reflect an advance of the Soldier Creek glacier

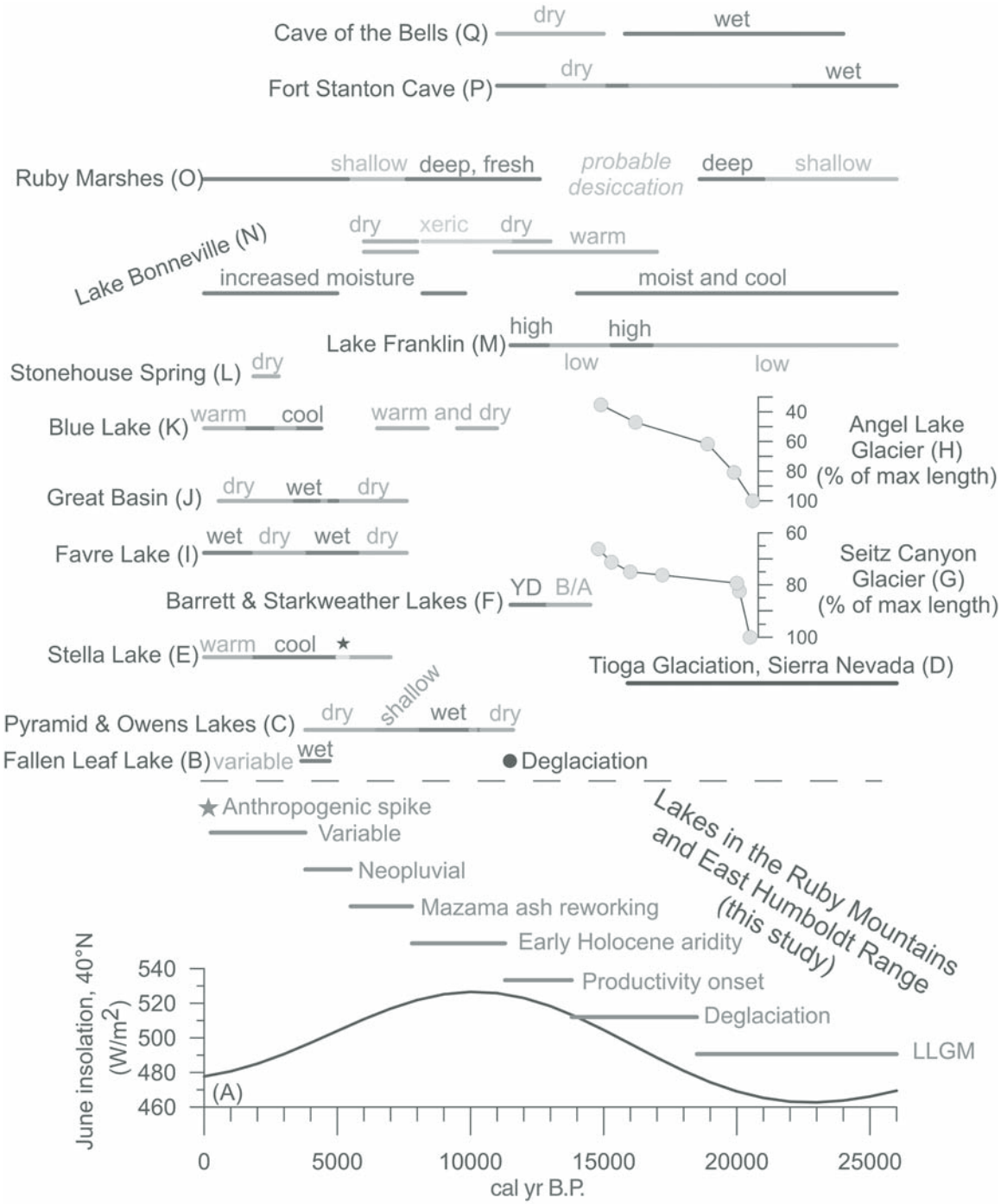


Figure 8. Compilation of results from the Ruby Mountains and East Humboldt Range lakes with other records from the Great Basin. (A) June 40°N insolation (Berger, 1978). LLGM—local Last Glacial Maximum. (B) Fallen Leaf Lake, Sierra Nevada (Noble et al., 2016). (C) Hydrography of Pyramid and Owens Lakes (Benson et al., 2002). (D) Sierra Nevada glacial advances from Owens Lake rock flour (Bischoff and Cummins, 2001). (E) Chironomid-inferred summer temperature reconstruction for Stella Lake, Nevada (Reinemann et al., 2009). Star marks peak warmth ca. 5.5 cal ka (F) Timing of the Younger Dryas (YD) and Bølling-Allerød (B/A) in Lake Barrett and Starkweather Lakes, Sierra Nevada (MacDonald et al., 2008). (G) Retreat of Seitz Canyon glacier, Ruby Mountains (Laabs et al., 2013). (H) Retreat of Angel Lake glacier, East Humboldt Range (Munroe et al., 2015). (I) Favre Lake, Ruby Mountains (Wahl et al., 2015). (J) Dry and wet periods in the Great Basin (Mensing et al., 2004, 2008). (K) Blue Lake, Utah (Louderback and Rhode, 2009). (L) Stonehouse Spring, Nevada (Benson et al., 2013). (M) Pluvial Lake Franklin (Munroe and Laabs, 2013a). (N) Lake Bonneville (Madsen et al., 2001; Oviatt, 1997). (O) Ruby Marshes, Nevada (Thompson, 1992). (P) Fort Stanton Cave, New Mexico (Asmerom et al., 2010; Polyak et al., 2012). (Q) Cave of the Bells, Arizona (Wagner et al., 2010).

in response to Heinrich event 2, ca. 24 cal ka (Hemming, 2004). However, the lack of tight age control through this interval precludes rigorous investigation of the timing and apparent periodicity of these peaks.

***Deglaciation (18.5–13.8 cal ka)***

Deglaciation of the Ruby Mountains and East Humboldt Range during the last glacial-interglacial transition is primarily recorded by the core from Soldier Lake (Fig. 6), although the very bottom of the Overland Lake core extends into this time interval (Fig. 5). Sediments accumulating during deglaciation in both lakes are characterized by high and consistent values of BD and % clastic, as well as low bSi, OM, and C:N. In Soldier Lake, sand abundance increased during this interval, while clay and silt decreased. The abundance of clay, in particular, dropped to ~2% ca. 18 cal ka and remained consistently low until rising rapidly at 13.6 cal ka. GS trends are more difficult to identify in Overland Lake without the ability to compare them with the preceding glacial interval.

The transition in Soldier Lake from sediment dominated by fine and very fine silt toward elevated (up to 25% of total) abundance of sand is consistent with increased fluvial transport of sediment to the lake basin as glacial meltwater enhanced stream power during ice retreat (Leonard, 1997). Values of median GS reach their highest sustained levels in the Soldier Lake record at this time, underscoring the uniqueness of this time interval (Fig. 6). Increased median GS and sand abundance may also reflect the onset of seasonal ice-free conditions at Soldier Lake and greater seasonal snowmelt in the surrounding watershed.

The calibrated basal age of 13.5 cal ka for the Overland Lake core provides a constraint on deglaciation because the lake could not have formed until after the glacier retreated to a position farther up valley. Given the position of Overland Lake relative to the terminal moraine, this retreat corresponds to an ~70% reduction in glacier length, and a rise in terminus elevation of ~500 m (70% of the drop from the headwall to the terminal moraine). Cosmogenic surface-exposure dating of glacially sculpted bedrock immediately up valley from Overland Lake yielded an age of 12,800 ± 700 yr B.P. (Sackett et al., 2016), consistent with the basal radiocarbon age reported here.

Retreat of the Soldier Creek and Overland Creek glaciers after ca. 18.5 cal ka is consistent with the timing of the last glacial-interglacial transition elsewhere in the Great Basin. Throughout this region, valley glaciers retreated from their terminal moraines after ca. 19 ka B.P., including in the Ruby Mountains and East Humboldt Range (Fig. 8; Munroe et al., 2015; Laabs et al., 2013), the Wasatch Mountains (Laabs et al., 2011), the western Uinta Mountains (Laabs et al., 2007, 2009), and the Sierra Nevada (Phillips et al., 2009; Rood et al., 2011; Phillips, 2016). Diatom records from Bear Lake (Utah and Idaho) indicate cold and turbid conditions from 19.1 to 13.8 cal ka due to an influx of meltwater from melting glaciers in the watershed (Moser and Kimball, 2009). Other lines of evidence indicate major changes in effective moisture during this interval. For instance, Lakes Bonneville and Franklin (Figs. 8M and 8N), and other pluvial lakes throughout the Great Basin, reached their maximum levels for the last pluvial cycle ca. 17 cal ka, synchronous with Heinrich event 1 in the North Atlantic region (Munroe and Laabs, 2013b). Speleothems from the southern Great Basin, and from along the California coast (Oster et al., 2015a; Oster et al., 2015b), also record changes in moisture amount and (possibly) source during the deglaciation interval. None of these speleothem records is in the immediate vicinity of the Ruby Mountains and East Humboldt Range; however, a compilation of available paleoclimate data suggests that a precipitation dipole dominated this region during deglaciation, with the northern Great Basin in a transition zone between a wetter southwest and a drier northwest (Oster et al., 2015a). Evolution of this dipole during deglaciation may have driven changes in effective moisture in the Great Basin.

Cosmogenic surface-exposure dating of recessional moraines in other valleys of the Ruby Mountains and East Humboldt Range reveals that glaciers paused and/or readvanced during overall retreat (Munroe et al., 2015; Laabs et al., 2013). The presence of these moraines suggests that the climatic trends responsible for deglaciation were not monotonic. A recessional moraine at the lip of a small basin ~200 m above Soldier Lake indicates that the Soldier Creek glacier also paused during overall retreat. However, once the glacier retreated from the terminal moraine, meltwater drainage was likely routed down the main valley axis, bypassing the basin where Soldier Lake is located. Thus, fluctuations in glacier retreat rate are not directly recorded in the sediments of Soldier Lake.

***Onset of Productivity (13.8–11.3 cal ka)***

The records from both Soldier and Overland Lakes document a rapid increase in organic productivity in the latest Pleistocene (Figs. 5, 6, and 7). During this interval, values of OM and C:N rise, while BD and % clastic decrease. MS remains fairly constant in both records. Median GS drops in Soldier Lake and stays relatively constant in Overland Lake. The abundance of bSi rises dramatically in Overland Lake, from starting values near the detection limit (~1%) up to ~20% by 12.0 cal ka. In contrast, values of bSi stay low (~1%) but have more variability during this interval in Soldier Lake. The apparent delay between the onset of rising bSi in these lakes may reflect fundamental differences in their bathymetry (Fig. 2), influencing the habitat available for benthic versus planktic diatoms.

The simultaneous increase of OM and C:N in both lakes signals a dramatic shift toward increased organic productivity within and around these lakes following deglaciation. A more productive lake environment would lead to more OM accumulating on the lake floor, and more terrestrial vegetation in the watershed (with a higher C:N) would also contribute to elevated OM levels in the lake sediment, as that material was transported to the lake. Furthermore, the small twig that produced the near-basal age of 13.5 cal ka for the Overland Lake core indicates the presence of woody vegetation in the watershed by that time. By the end of this interval, ca. 11.3 cal ka, OM abundance in both lakes

had risen to mean values for the postglacial period, suggesting establishment of a near-modern vegetation density.

Rapid onset of organic productivity following deglaciation is a hallmark of many lacustrine records from mountain areas in the western United States. In the Uinta Mountains, for instance, study of numerous lacustrine records has indicated a similarly abrupt rise in OM in the latest Pleistocene and early Holocene (Munroe, 2007; Corbett and Munroe, 2010; Tingstad et al., 2011; Munroe and Laabs, 2017). Downstream from the northwestern Uinta Mountains, diatoms record warmer and less turbid water in Bear Lake starting at 13.8 cal ka (Moser and Kimball, 2009). The onset of organic productivity in Fallen Leaf Lake, near Lake Tahoe at the western edge of the Great Basin, occurred ca. 11.5 cal ka (Noble et al., 2016). In Colorado to the east, organic values in Cumbres Bog (Johnson et al., 2013) and Bison Lake (Anderson et al., 2015) rose during this same interval.

Many paleoclimate records from this time record cooling or other climatic aberrations associated with the Younger Dryas (YD) event (Fairbanks, 1990; Alley, 2000). This event primarily impacted the North Atlantic region (Carlson et al., 2007), but paleoclimate records from throughout the northern midlatitudes contain evidence of climate shifts potentially related to YD cooling. For instance, in the Rocky Mountains, residual alpine glaciers may have advanced in response to the YD (Gosse et al., 1995). Glaciers in the Sierra Nevada apparently advanced earlier, ca. 13 ka B.P., during the Recess Peak glaciation (Phillips et al., 2009; Phillips, 2016); however, lacustrine records from the Sierra Nevada indicate climatic cooling associated with the YD (MacDonald et al., 2008). The lingering remnant of pluvial Lake Bonneville transgressed during the latest Pleistocene, perhaps in response to the YD (Oviatt et al., 2005), as did pluvial Lake Franklin in the Ruby Marshes (Fig. 8M; Munroe and Laabs, 2013a), Lake Lahontan (Benson et al., 2013), and Lake Chewaucan (Licciardi, 2001). Some proxies in the Overland and Soldier Lake cores exhibit distinct behavior during the YD. In Overland Lake, values of C:N drop and remain low during the YD, coincident with an interruption in rising bSi values (Fig. 5). In both lakes, the abundance of OM rises much faster after the YD ends ca. 11.7 cal ka (Figs. 5 and 6). Overall, however, evidence for a YD-related climate shift in the Overland and Soldier Lake records is equivocal.

***Early Holocene Aridity (11.3–7.8 cal ka)***

Both Overland and Soldier Lakes contain evidence of lowered water levels and aridity in the early Holocene (Figs. 5, 6, and 7). Values of OM and C:N are synchronously above average during the interval 11.3–7.8 cal ka. Abundance of bSi in the Soldier Lake core remains low, but bSi in Overland Lake is near a maximum at this time. Values of % clastic and MS are low in both lakes. The GS distribution within the Overland Lake record is relatively consistent. Sand abundance in Solder Lake is near maximum values for part of this interval, but it drops dramatically ca. 8.0 cal ka. Together, these proxy shifts are consistent with a situation in which water levels in these lakes were low, moving the littoral zone closer to the coring site, and facilitating the transport of coarser clastic sediment, and greater amounts of terrestrially derived OM, to the lake depocenter (e.g., Shuman, 2003).

Low water levels at this time are synchronous with the summer insolation maximum for this latitude (Fig. 8A), which is consistent with elevated summer temperatures. Previous studies have also interpreted bSi as a proxy for summer temperatures (McKay et al., 2008). Therefore, the record-high bSi values in Overland Lake could be a signal of warm summers in the earliest Holocene. Similar warm and dry conditions in the northwestern Great Basin between 11 and 9 cal ka were inferred from pollen and charcoal (Minckley et al., 2007). Other regional evidence indicates that climate at lower elevations was dry at this time. For instance, information from woodrat middens records the expansion of sagebrush in response to drier conditions between 11.5 and 8.2 cal ka (Rhode and Madsen, 1995; Madsen et al., 2001), and Owens Lake in the western Great Basin experienced a drying trend between 11.6 and 10.0 cal ka (Fig. 8C; Benson et al., 2002). Similarly, at Blue Lake, ~100 km east of the Ruby Mountains and East Humboldt Range, paleobotanical data indicate aridification after ca. 11 cal ka, culminating ca. 9.5 cal ka (Fig. 8K; Louderback and Rhode, 2009).

***Tephra Reworking (7.8–5.5 cal ka)***

Almost all paleoclimate proxies investigated in this study were impacted by deposition and reworking of tephra associated with the climactic eruption of Mount Mazama at 7.6 ka B.P. (Zdanowicz et al., 1999). The core retrieved from Angel Lake bottomed in a Mazama ash layer of unknown thickness, whereas both the Overland and Solider Lake cores penetrated through the Mazama ash (Fig. 3). In Overland Lake, the primary tephra layer (8 cm thick) was overlain by 10 cm of reworked ash, distinguished by swirls of incorporated OM. In Soldier Lake, the primary tephra layer was 4 cm thick, with an overlying 5 cm section of mixed tephra and organic sediment. The deposition of this layer of ash presumably had considerable consequences for the watersheds of these lakes, both in the immediate aftermath of the eruption and over the following years as tephra was remobilized across the landscape (e.g., Long et al., 2014). Measured values of OM and C:N fall after ash deposition, and median GS, sand abundance, MS, and bSi generally rise (Figs. 4, 5, and 6). However, these changes are more likely evidence of tephra reworking rather than paleoclimate variability. Dilution of organic sediment in the lake with ash explains the lowered organic content. A higher abundance of Fe-bearing grains in the ash would lead to elevated MS values after the eruption. Because the ash is generally coarser than the local sediment that was accumulating in the lakes at this time, median GS and sand abundance would increase following deposition. Elevated bSi values can be attributed to dissolution of amorphous silica-bearing volcanic glass by the hot NaOH leach method used to quantify bSi.

Overall, the Mazama ash layer provides a solid chronologic tie point among the three records and strengthens the age models

for the individual lakes, yet reworking of this ash in the centuries following its deposition obscures other paleoenvironmental signals in the studied proxies. It is worth noting, however, that study of diatom assemblages in Favre Lake in the Ruby Mountains (Wahl et al., 2015) has revealed that low water levels continued until ca. 5.8 cal ka (Fig. 8I), and the Ruby Marshes (Thompson, 1992), Pyramid and Owens Lakes (Benson et al., 2002) apparently became more shallow at this time (Fig. 8C). Conditions were also warm and dry (Fig. 8K) at Blue Lake (Louderback and Rhode, 2009) and other sites throughout the Great Basin (Mensing et al., 2004, 2008). The frequency of coarse layers in the Angel Lake core (Fig. 4) also rose to a peak around 5.5 cal ka. Because the coring site at Angel Lake was intentionally selected to avoid the deep hole immediately adjacent to the inlet (Fig. 2), it seems unlikely that these coarse layers reflect floods of the inlet stream. Rather, delivery of coarse sediment to the coring site is consistent with high-energy transport of coarse material onto the frozen lake surface through snow avalanching or slush flows during snowmelt. Relatively frequent coarse layers in the middle Holocene might, therefore, be a sign of rapid springtime warming and snowmelt.

***Neopluvial (5.5–3.8 cal ka)***

The interval following the dwindling influence of ash reworking features proxy shifts that provide evidence of wetter conditions (Figs. 4, 5, and 6). In Soldier Lake, bSi finally begins to rise rapidly toward maximum values (Fig. 6). The ratio of C:N also rises, while the abundance of sand decreases. Collectively, these shifts record a rise in water levels leading to an expanded lake surface area. Because no major streams enter Soldier Lake from its small watershed, migration of the shoreline away from the lake center would reduce the amount of coarse clastic sediment arriving at the coring site. Flooding of the shallow shelf surrounding the depocenter (Fig. 2) would have provided additional habitat for benthic diatoms, which could be reflected in the increasing bSi values. Erosion of surrounding soils by rising lake waters would have liberated OM with a relatively higher C:N ratio for redistribution within the lake.

Median GS, C:N, and MS values rise at the same time in Overland Lake (Fig. 5). Because Overland Lake is fed by a stream draining a higher cirque, these changes are consistent with a sustained increase in the volume of streamwater entering the lake. Lake level may not have risen in conjunction with this hydrologic shift because water can easily exit the lake over the sill at the northern end of the basin. A similar situation exists at Angel Lake, where the frequency of coarse layers began to decline, but remained above average during this interval (Fig. 4). Values of C:N were also relatively high in Angel Lake, signaling delivery of terrestrial OM eroded from the wetlands upstream of the lake.

Abundant evidence indicates that hydroclimate in the Great Basin shifted broadly toward wetter conditions during a neopluvial interval ca. 5.0–3.8 cal ka (e.g., Noble et al., 2016). In the Ruby Mountains (Fig. 8I), diatom evidence reveals wetter conditions at Favre Lake from 5.5 to 3.8 cal ka (Wahl et al., 2015). In the Sierra Nevada, water levels rose in Fallen Leaf Lake (Fig. 8B; Noble et al., 2016). Chironomid-inferred summer temperatures reached peak values at Stella Lake ca. 5.5 cal ka (Fig. 8E), after which cooler conditions dominated (Reinemann et al., 2009). At lower elevations, Walker Lake began to rise at ca. 4.7 cal ka (Benson et al., 1991; Adams, 2007), pollen provides evidence of wetter conditions in the Ruby Marshes (Fig. 8O; Thompson, 1992), salinity decreased in the Great Salt Lake (Madsen et al., 2001), and conditions were cooler at Blue Lake (Fig. 8K; Louderback and Rhode, 2009).

***Variable Climate (3.8 ka–250 yr B.P.)***

Beginning around 3.8 cal ka, proxies in the studied lakes shift in directions indicating a more variable late Holocene climate. In both Soldier and Overland Lakes, OM levels abruptly jump to maximum values (Fig. 7). Values of C:N drop, indicating that more of this OM was of aquatic origin. In this interval, values of bSi were at or near the maximum in Soldier Lake, and tended to be above average in the other lakes as well. Sand abundance decreased in Soldier Lake (Fig. 6), whereas median GS rose in Overland Lake (Fig. 5). The frequency of coarse layers in Angel Lake remained below average from 3.8 to 1.8 cal ka, although the median GS of these layers increased (Fig. 4). After ca. 1.0 cal ka, coarse layer frequency was above average again. Collectively, these proxy trends are not easily explained by an overall, consistent shift toward wetter or drier conditions. Rather, they represent climatic variability filtered by the unique characteristics of each lake and its watershed (Table 1).

Other studies from the region have noted evidence for variable climatic conditions during the late Holocene. Noble et al. (2016) documented an increase in clastic sedimentation and a decrease in bSi in Fallen Leaf Lake at the western end of the Great Basin (Fig. 8B), and they suggested that this pattern signals a shift to drier winter conditions. Similarly, diatom evidence indicates dry conditions at Favre Lake (Fig. 8I) from 3.8 to 1.8 cal ka (Wahl et al., 2015). In contrast, chironomid-inferred summer temperatures were cooler at Stella Lake (Fig. 8E) from 4.2 to 1.0 cal ka (Reinemann et al., 2009), and water depths increased at Ruby Marsh (Fig. 8O; Thompson, 1992). Climatic conditions were variable at Blue Lake (Fig. 8K; Louderback and Rhode, 2009), and the Great Salt Lake became fresh enough to support Utah chub, a moderately salt-tolerant species, at ca. 3.4 and ca. 1.2 cal ka (Madsen et al., 2001). Variability at submillennial time scales is also illustrated by rooted trees submerged in Fallen Leaf Lake that have drowning dates clustering around 1.8 and 0.75 cal ka (Noble et al., 2016). Signs of a regional dry episode between 2.8 and 1.85 cal ka have also been compiled (Mensing et al., 2013), providing additional evidence for dramatic shifts in hydroclimate during the late Holocene.

***Anthropogenic Spike (250 yr B.P. to Present)***

Precision of the $^{14}$C-based age models likely decreases in the uppermost sediments from each lake because of nonlinear

changes in density within the relatively uncompacted core-top sediments (Fig. 3). Nonetheless, it is notable that proxies in all three lakes exhibit dramatic shifts at depths corresponding to the last century or two. Typically, values of bSi rise, OM rises considerably, and C:N falls to at or near minimum levels (Fig. 7). Collectively, these shifts signify a synchronous change toward increased in-lake productivity, greater algal growth, and reduced importance of terrestrial OM. This shift may have been driven by a lengthening of the ice-free season and/or increased summer water temperatures, permitting greater diatom growth. Elevated chironomid-inferred summer water temperatures in the past few centuries have been reconstructed for other Great Basin lakes (Reinemann et al., 2009; Porinchu et al., 2010). Alternatively, these changes could be a result of increased delivery of nutrient-bearing dust liberated from surrounding lowlands by anthropogenic disturbance. Lake sediment records in Utah and Colorado contain evidence of anthropogenic changes in dust delivery over the past few centuries that have impacted high-elevation environments (Neff et al., 2008; Moser et al., 2010; Reynolds et al., 2010).

## CONCLUSION

Sediment cores retrieved from three lakes at high elevations in the Ruby Mountains and East Humboldt Range of northeastern Nevada provide a comprehensive record of climatic and environmental changes over the past 26,000 yr. Soldier Lake, located just beyond the terminal moraine of the Angel Lake glaciation, accumulated inorganic rock flour during the local Last Glacial Maximum and records an onset of deglaciation ca. 18.5 cal ka, consistent with surface-exposure ages on moraines elsewhere in the region. Both Soldier and Overland Lakes record a rapid increase in organic productivity between 13.8 and 11.3 cal ka, essentially synchronous with lakes in similar mountain settings elsewhere in the southwestern United States. Soldier and Overland Lakes record an episode of low water levels in the early Holocene, likely correlated with the summer insolation maximum. Deposition and reworking of the Mazama ash in the middle Holocene obscure environmental signals from the proxies for ~1.5 k.y.; however, records from elsewhere in the region indicate peak aridity and low water levels at this time. Neopluvial conditions, associated with enhanced hydrologic throughflow and rising water levels existed between 5.5 and 3.8 cal ka, matching records of increased effective moisture elsewhere in the Great Basin. Climatic conditions became more variable after 3.8 cal ka, with evidence for submillennial shifts in hydroclimate and sediment inwashing. Finally, although imprecision in the depth-age models precludes a direct assessment of the timing, all three lakes record dramatic increases in organic content and biogenic silica synchronous with profound drops in C:N ratio during the past century or two. These changes may reflect climatic warming following the Neoglaciation, or elevated nutrient status in response to enhanced delivery of eolian dust due to anthropogenic activity in the surrounding lowlands.

## ACKNOWLEDGMENTS

Permission to work in the Ruby Mountains and East Humboldt Range was provided by the Humboldt-Toiyabe National Forest. The core from Soldier Lake was collected by D. Porinchu and S. Reinemann. The field assistance of N. Taylor was critical for the coring efforts at Overland Lake. Mazama ash in the cores from Overland and Soldier Lakes was identified by E. Wan and D. Wahl with the U.S. Geological Survey Tephrachronology Project. Support for this project was provided by National Science Foundation grants EAR-0902586 and MRI-0922940 to J. Munroe. M. Bigl and A. Silverman received support from Middlebury College. Thoughtful comments by S. Starratt, M. Rosen, C. Koeberl, and two anonymous reviewers are appreciated.

## REFERENCES CITED

Adams, K.D., 2007, Late Holocene sedimentary environments and lake-level fluctuations at Walker Lake, Nevada, USA: Geological Society of America Bulletin, v. 119, p. 126–139, https://doi.org/10.1130/B25847.1.

Alley, R.B., 2000, The Younger Dryas cold interval as viewed from central Greenland: Quaternary Science Reviews, v. 19, p. 213–226, https://doi.org/10.1016/S0277-3791(99)00062-1.

Anderson, L., Brunelle, A., and Thompson, R.S., 2015, A multi-proxy record of hydroclimate, vegetation, fire, and post-settlement impacts for a subalpine plateau, central Rocky Mountains, U.S.A.: The Holocene, v. 25, p. 932–943, https://doi.org/10.1177/0959683615574583.

Asmerom, Y., Polyak, V.J., and Burns, S.J., 2010, Variable winter moisture in the southwestern United States linked to rapid glacial climate shifts: Nature Geoscience, v. 3, p. 114–117, https://doi.org/10.1038/ngeo754.

Benson, L., Meyers, P.A., and Spencer, R., 1991, Change in the size of Walker Lake during the past 5000 years: Palaeogeography, Palaeoclimatology, Palaeoecology, v. 81, p. 189–214, https://doi.org/10.1016/0031-0182(91)90147-J.

Benson, L., Kashgarian, M., Rye, R.O., Lund, S.P., Paillet, F.L., Smoot, J.P., Kester, C.L., Mensing, S., Meko, D., and Lindstrom, S., 2002, Holocene multidecadal and multicentennial droughts affecting Northern California and Nevada: Quaternary Science Reviews, v. 21, p. 659–682, https://doi.org/10.1016/S0277-3791(01)00048-8.

Benson, L., Smoot, J., Lund, S., Mensing, S., Foit, F., Jr., and Rye, R., 2013, Insights from a synthesis of old and new climate-proxy data from the Pyramid and Winnemucca lake basins for the period 48 to 11.5 cal ka: Quaternary International, v. 310, p. 62–82, https://doi.org/10.1016/j.quaint.2012.02.040.

Berger, A.L., 1978, Long-term variations of caloric insolation resulting from the Earth's orbital elements: Quaternary Research, v. 9, p. 139–167, https://doi.org/10.1016/0033-5894(78)90064-9.

Bischoff, J.L., and Cummins, K., 2001, Wisconsin glaciation of the Sierra Nevada (79,000–15,000 yr B.P.) as recorded by rock flour in sediments of Owens Lake, California: Quaternary Research, v. 55, p. 14–24, https://doi.org/10.1006/qres.2000.2183.

Blaauw, M., 2010, Methods and code for 'classical' age-modelling of radiocarbon sequences: Quaternary Geochronology, v. 5, p. 512–518, https://doi.org/10.1016/j.quageo.2010.01.002.

Carlson, A.E., Clark, P.U., Haley, B.A., Klinkhammer, G.P., Simmons, K., Brook, E.J., and Meissner, K.J., 2007, Geochemical proxies of North American freshwater routing during the Younger Dryas cold event: Proceedings of the National Academy of Sciences of the United States of America, v. 104, p. 6556–6561, https://doi.org/10.1073/pnas.0611313104.

Clark, P.U., Dyke, A.S., Shakun, J.D., Carlson, A.E., Clark, J., Wohlfarth, B., Mitrovica, J.X., Hostetler, S.W., and McCabe, A.M., 2009, The Last Glacial Maximum: Science, v. 325, p. 710–714, https://doi.org/10.1126/science.1172873.

Corbett, L.B., and Munroe, J.S., 2010, Investigating the influence of hydrogeomorphic setting on the response of lake sedimentation to climatic changes in the Uinta Mountains, Utah, USA: Journal of Paleolimnology, v. 44, p. 311–325, https://doi.org/10.1007/s10933-009-9405-9.

Dean, W.E., Jr., 1974, Determination of carbonate and organic matter in calcareous sediments and sedimentary rocks by loss on ignition; comparison with other methods: Journal of Sedimentary Petrology, v. 44, p. 242–248.

DeMaster, D.J., 1981, The supply and accumulation of silica in the marine environment: Geochimica et Cosmochimica Acta, v. 45, p. 1715–1732, https://doi.org/10.1016/0016-7037(81)90006-5.

Fairbanks, R.G., 1990, The age and origin of the "Younger Dryas climate event" in Greenland ice cores: Paleoceanography, v. 5, p. 937–948, https://doi.org/10.1029/PA005i006p00937.

Gosse, J.C., Evenson, E.B., Klein, J., Lawn, B., and Middleton, R., 1995, Precise cosmogenic $^{10}$Be measurements in western North America; support for a global Younger Dryas cooling event: Geology, v. 23, p. 877–880, https://doi.org/10.1130/0091-7613(1995)023<0877:PCBMIW>2.3.CO;2.

Grayson, D., 2011, The Great Basin: A Natural Prehistory: Berkeley, California, University of California Press, 432 p.

Hemming, S.R., 2004, Heinrich events; massive late Pleistocene detritus layers of the North Atlantic and their global climate imprint: Reviews of Geophysics, v. 42, RG1005.1–RG1005.43.

Johnson, B.G., Jiménez-Moreno, G., Eppes, M.C., Diemer, J.A., and Stone, J.R., 2013, A multiproxy record of postglacial climate variability from a shallowing, 12-m deep sub-alpine bog in the southeastern San Juan Mountains of Colorado, USA: The Holocene, v. 23, p. 1028–1038, https://doi.org/10.1177/0959683613479682.

Laabs, B.J.C., Munroe, J.S., Rosenbaum, J.G., Refsnider, K.A., Mickelson, D.M., Singer, B.S., and Caffee, M.W., 2007, Chronology of the Last Glacial Maximum in the upper Bear River Basin, Utah: Arctic, Antarctic, and Alpine Research, v. 39, p. 537–548, https://doi.org/10.1657/1523-0430(06-089)[LAABS]2.0.CO;2.

Laabs, B.J.C., Refsnider, K.A., Munroe, J.S., Mickelson, D.M., Applegate, P.J., Singer, B.S., and Caffee, M.W., 2009, Latest Pleistocene glacial chronology of the Uinta Mountains: Support for moisture-driven asynchrony of the last deglaciation: Quaternary Science Reviews, v. 28, p. 1171–1187, https://doi.org/10.1016/j.quascirev.2008.12.012.

Laabs, B.J., Marchetti, D.W., Munroe, J.S., Refsnider, K.A., Gosse, J.C., Lips, E.W., Becker, R.A., Mickelson, D.M., and Singer, B.S., 2011, Chronology of latest Pleistocene mountain glaciation in the western Wasatch Mountains, Utah, U.S.A.: Quaternary Research, v. 76, p. 272–284, https://doi.org/10.1016/j.yqres.2011.06.016.

Laabs, B.J.C., Munroe, J.S., Best, L.C., and Caffee, M.W., 2013, Timing of the last glaciation and subsequent deglaciation in the Ruby Mountains, Great Basin, USA: Earth and Planetary Science Letters, v. 361, p. 16–25, https://doi.org/10.1016/j.epsl.2012.11.018.

Leonard, E.M., 1997, The relationship between glacial activity and sediment production; evidence from a 4450-year varve record of neoglacial sedimentation in Hector Lake, Alberta, Canada: Journal of Paleolimnology, v. 17, p. 319–330, https://doi.org/10.1023/A:1007948327654.

Licciardi, J.M., 2001, Chronology of latest Pleistocene lake-level fluctuations in the pluvial Lake Chewaucan basin, Oregon, USA: Journal of Quaternary Science, v. 16, p. 545–553, https://doi.org/10.1002/jqs.619.

Livingstone, D.A., 1955, A lightweight piston sampler for lake deposits: Ecology, v. 36, p. 137–139, https://doi.org/10.2307/1931439.

Long, C.J., Power, M.J., Minckley, T.A., and Hass, A.L., 2014, The impact of Mt. Mazama tephra deposition on forest vegetation in the Central Cascades, Oregon, USA: The Holocene, v. 24, p. 503–511, https://doi.org/10.1177/0959683613520258.

Louderback, L.A., and Rhode, D.E., 2009, 15,000 years of vegetation change in the Bonneville Basin; the Blue Lake pollen record: Quaternary Science Reviews, v. 28, p. 308–326, https://doi.org/10.1016/j.quascirev.2008.09.027.

MacDonald, G.M., Moser, K., Bloom, A.M., Porinchu, D.F., Potito, Wolfe, B.B., Edwards, T., Petel, A., Orme, A.R., and Orme, A.J., 2008, Evidence of temperature depression and hydrological variations in the eastern Sierra Nevada during the Younger Dryas stade: Quaternary Research, v. 70, p. 131–140, https://doi.org/10.1016/j.yqres.2008.04.005.

Madsen, D.B., Rhode, D., Grayson, D.K., Broughton, J.M., Livingston, S.D., Hunt, J., Quade, J., Schmitt, D.N., and Shaver, M.W., 2001, Late Quaternary environmental change in the Bonneville Basin, western USA: Palaeogeography, Palaeoclimatology, Palaeoecology, v. 167, p. 243–271, https://doi.org/10.1016/S0031-0182(00)00240-6.

McKay, N.P., Kaufman, D.S., and Michelutti, N., 2008, Biogenic silica concentration as a high-resolution, quantitative temperature proxy at Hallet Lake, south-central Alaska: Geophysical Research Letters, v. 35, no. 5, L05709, https://doi.org/10.1029/2007GL032876.

Menounos, B., 1997, The water content of lake sediments and its relationship to other physical parameters: An alpine case study: The Holocene, v. 7, p. 207–212, https://doi.org/10.1177/095968369700700208.

Mensing, S.A., Benson, L.V., Kashgarian, M., and Lund, S., 2004, A Holocene pollen record of persistent droughts from Pyramid Lake, Nevada, USA: Quaternary Research, v. 62, p. 29–38, https://doi.org/10.1016/j.yqres.2004.04.002.

Mensing, S.A., Smith, J., Burkle, N.K., and Allan, M., 2008, Extended drought in the Great Basin of western North America in the last two millennia reconstructed from pollen records: Quaternary International, v. 188, p. 79–89, https://doi.org/10.1016/j.quaint.2007.06.009.

Mensing, S.A., Sharpe, S.E., Tunno, I., Sada, D.W., Thomas, J.M., Starratt, S., and Smith, J., 2013, The late Holocene dry period: Multiproxy evidence for an extended drought between 2800 and 1850 cal yr B.P. across the central Great Basin, USA: Quaternary Science Reviews, v. 78, p. 266–282, https://doi.org/10.1016/j.quascirev.2013.08.010.

Meyers, P.A., and Ishiwatari, R., 1993, Lacustrine organic geochemistry; an overview of indicators of organic matter sources and diagenesis in lake sediments: Organic Geochemistry, v. 20, p. 867–900, https://doi.org/10.1016/0146-6380(93)90100-P.

Mifflin, M.D., and Wheat, M.M., 1979, Pluvial Lakes and Estimated Pluvial Climates of Nevada: Nevada Bureau of Mines and Geology Bulletin 94, 60 p.

Minckley, T.A., Whitlock, C., and Bartlein, P.J., 2007, Vegetation, fire, and climate history of the northwestern Great Basin during the last 14,000 years: Quaternary Science Reviews, v. 26, p. 2167–2184, https://doi.org/10.1016/j.quascirev.2007.04.009.

Moser, K.A., and Kimball, J.P., 2009, A 19,000-year record of hydrologic and climatic change inferred from diatoms from Bear Lake, Utah and Idaho, *in* Rosenbaum, J.G., and Kaufman, D.S., eds., Paleoenvironments of Bear Lake, Utah and Idaho, and Its Catchment: Geological Society of America Special Paper 450, p. 229–246.

Moser, K.A., Mordecai, J.S., Reynolds, R.L., Rosenbaum, J.G., and Ketterer, M.E., 2010, Diatom changes in two Uinta Mountain lakes, Utah, USA: Responses to anthropogenic and natural atmospheric inputs: Hydrobiologia, v. 648, p. 91–108, https://doi.org/10.1007/s10750-010-0145-7.

Munroe, J.S., 2007, Exploring relationships between watershed properties and Holocene loss-on-ignition records in high-elevation lakes, southern Uinta Mountains, Utah, U.S.A.: Arctic, Antarctic, and Alpine Research, v. 39, p. 556–565, https://doi.org/10.1657/1523-0430(06-096)[MUNROE]2.0.CO;2.

Munroe, J.S., and Laabs, B.J.C., 2011, New investigations of Pleistocene glacial and pluvial records in northeastern Nevada, *in* Lee, J., and Evans, J.P., eds., Geologic Field Trips to the Basin and Range, Rocky Mountains, Snake River Plain, and Terranes of the U.S. Cordillera: Geological Society of America Field Guide 21, p. 1–25, https://doi.org/10.1130/2011.0021(01).

Munroe, J.S., and Laabs, B.J., 2013a, Latest Pleistocene history of pluvial Lake Franklin, northeastern Nevada, USA: Geological Society of America Bulletin, v. 125, p. 322–342, https://doi.org/10.1130/B30696.1.

Munroe, J.S., and Laabs, B.J., 2013b, Temporal correspondence between pluvial lake highstands in the southwestern US and Heinrich event 1: Journal of Quaternary Science, v. 28, p. 49–58, https://doi.org/10.1002/jqs.2586.

Munroe, J.S., and Laabs, B.J., 2017, Combining radiocarbon and cosmogenic ages to constrain the timing of the last glacial-interglacial transition in the Uinta Mountains, Utah, USA: Geology, v. 45, p. 171–174, https://doi.org/10.1130/G38156.1.

Munroe, J.S., Laabs, B.J.C., Shakun, J.D., Singer, B.S., Mickelson, D.M., Refsnider, K.A., and Caffee, M.W., 2006, Latest Pleistocene advance of alpine glaciers in the southwestern Uinta Mountains, Utah, USA: Evidence for the influence of local moisture sources: Geology, v. 34, p. 841–844, https://doi.org/10.1130/G22681.1.

Munroe, J.S., Laabs, B.J.C., Oviatt, C.G., and Jewell, P.W., 2015, New investigations of Pleistocene pluvial and glacial records from the northeastern Great Basin, *in* Rosen, M.R., compiler, Sixth International Limnogeology Congress Field Trip Guidebook (Reno, Nevada, June 15–19, 2015): Reston, Virginia, U.S. Geological Survey, p. 1–30.

Neff, J.C., Ballantyne, A.P., Farmer, G.L., Mahowald, N.M., Conroy, J.L., Landry, C.C., Overpeck, J.T., Painter, T.H., Lawrence, C.R., and Reynolds, R.L., 2008, Increasing eolian dust deposition in the western United States linked to human activity: Nature Geoscience, v. 1, p. 189–195, https://doi.org/10.1038/ngeo133.

Noble, P.J., Ball, G.I., Zimmerman, S.H., Maloney, J., Smith, S.B., Kent, G., Adams, K.D., Karlin, R.E., and Driscoll, N., 2016, Holocene paleoclimate history of Fallen Leaf Lake, CA, from geochemistry and sedimentology of well-dated sediment cores: Quaternary Science Reviews, v. 131, p. 193–210, https://doi.org/10.1016/j.quascirev.2015.10.037.

Osborn, G., and Bevis, K., 2001, Glaciation in the Great Basin of the Western United States: Quaternary Science Reviews, v. 20, p. 1377–1410, https://doi.org/10.1016/S0277-3791(01)00002-6.

Oster, J.L., Ibarra, D.E., Winnick, M.J., and Maher, K., 2015a, Steering of westerly storms over western North America at the Last Glacial Maximum: Nature Geoscience, v. 8, p. 201–205, https://doi.org/10.1038/ngeo2365.

Oster, J.L., Montañez, I.P., Santare, L.R., Sharp, W.D., Wong, C., and Cooper, K.M., 2015b, Stalagmite records of hydroclimate in central California during termination 1: Quaternary Science Reviews, v. 127, p. 199–214, https://doi.org/10.1016/j.quascirev.2015.07.027.

Oviatt, C.G., 1997, Lake Bonneville fluctuations and global climate change: Geology, v. 25, p. 155–158, https://doi.org/10.1130/0091-7613(1997)025<0155:LBFAGC>2.3.CO;2.

Oviatt, C.G., 2015, Chronology of Lake Bonneville, 30,000 to 10,000 yr B.P.: Quaternary Science Reviews, v. 110, p. 166–171, https://doi.org/10.1016/j.quascirev.2014.12.016.

Oviatt, C.G., Miller, D.M., McGeehin, J.P., Zachary, C., and Mahan, S., 2005, The Younger Dryas phase of Great Salt Lake, Utah, USA: Palaeogeography, Palaeoclimatology, Palaeoecology, v. 219, p. 263–284, https://doi.org/10.1016/j.palaeo.2004.12.029.

Phillips, F.M., 2016, Cosmogenic nuclide data sets from the Sierra Nevada, California, for assessment of nuclide production models: I: Late Pleistocene glacial chronology: Quaternary Geochronology, v. 35, p. 119–129, https://doi.org/10.1016/j.quageo.2015.12.003.

Phillips, F.M., Zreda, M., Plummer, M.A., Elmore, D., and Clark, D.H., 2009, Glacial geology and chronology of Bishop Creek and vicinity, eastern Sierra Nevada, California: Geological Society of America Bulletin, v. 121, p. 1013–1033, https://doi.org/10.1130/B26271.1.

Poage, M., and Chamberlain, C., 2002, Stable isotopic evidence for a pre–middle Miocene rain shadow in the western Basin and Range: Implications for the paleotopography of the Sierra Nevada: Tectonics, v. 21, no. 4, p. 16-1–16-10, https://doi.org/10.1029/2001TC001303.

Polyak, V.J., Asmerom, Y., Burns, S.J., and Lachniet, M.S., 2012, Climatic backdrop to the terminal Pleistocene extinction of North American mammals: Geology, v. 40, p. 1023–1026, https://doi.org/10.1130/G33226.1.

Porinchu, D.F., Reinemann, S., Mark, B.G., Box, J.E., and Rolland, N., 2010, Application of a midge-based inference model for air temperature reveals evidence of late-20th century warming in sub-alpine lakes in the central Great Basin, United States: Quaternary International, v. 215, p. 15–26, https://doi.org/10.1016/j.quaint.2009.07.021.

Reasoner, M.A., 1993, Equipment and procedure improvements for a lightweight, inexpensive, percussion core sampling system: Journal of Paleolimnology, v. 8, p. 273–281, https://doi.org/10.1007/BF00177859.

Reimer, P.J., Bard, E., Bayliss, A., Beck, J.W., Blackwell, P.G., Bronk, R.C., Buck, C.E., Cheng, H., Edwards, R.L., and Friedrich, M., 2013, IntCal13 and Marine13 radiocarbon age calibration curves 0–50,000 years cal B.P.: Radiocarbon, v. 55, p. 1869–1887, https://doi.org/10.2458/azu_js_rc.55.16947.

Reinemann, S.A., Porinchu, D.F., Bloom, A.M., Mark, B.G., and Box, J.E., 2009, A multi-proxy paleolimnological reconstruction of Holocene climate conditions in the Great Basin, United States: Quaternary Research, v. 72, p. 347–358, https://doi.org/10.1016/j.yqres.2009.06.003.

Reynolds, R.L., Mordecai, J.S., Rosenbaum, J.G., Ketterer, M.E., Walsh, M.K., and Moser, K.A., 2010, Compositional changes in sediments of subalpine lakes, Uinta Mountains (Utah): Evidence for the effects of human activity on atmospheric dust inputs: Journal of Paleolimnology, v. 44, p. 161–175, https://doi.org/10.1007/s10933-009-9394-8.

Rhode, D., and Madsen, D.B., 1995, Late Wisconsin/early Holocene vegetation in the Bonneville Basin: Quaternary Research, v. 44, p. 246–256, https://doi.org/10.1006/qres.1995.1069.

Rood, D.H., Burbank, D.W., and Finkel, R.C., 2011, Chronology of glaciations in the Sierra Nevada, California, from $^{10}$Be surface exposure dating: Quaternary Science Reviews, v. 30, p. 646–661, https://doi.org/10.1016/j.quascirev.2010.12.001.

Sackett, H., Laabs, B.J., Munroe, J.S., and Eckes, S., 2016, Climate change during deglaciation of the Overland Creek Valley, Ruby Mountains, Nevada, USA: Geological Society of America Abstracts with Programs, v. 48, no. 2, https://doi.org/10.1130/abs/2016NE-272821.

Sharp, R.P., 1938, Pleistocene glaciation in the Ruby–East Humboldt Range, northeastern Nevada: Journal of Geomorphology, v. 1, p. 296–323.

Sharp, R.P., 1940, Geomorphology of the Ruby–East Humboldt Range, Nevada: Geological Society of America Bulletin, v. 51, p. 337–371, https://doi.org/10.1130/GSAB-51-337.

Shuman, B., 2003, Controls on loss-on-ignition variation in cores from two shallow lakes in the northeastern United States: Journal of Paleolimnology, v. 30, p. 371–385, https://doi.org/10.1023/B:JOPL.0000007226.68831.e3.

Stewart, J.H., 1971, Basin and Range structure: A system of horsts and grabens produced by deep-seated extension: Geological Society of America Bulletin, v. 82, p. 1019–1044, https://doi.org/10.1130/0016-7606(1971)82[1019:BARSAS]2.0.CO;2.

Strickland, J.D.H., and Parsons, T.R., 1965, A Manual of Sea Water Analysis, with Special Reference to the More Common Micronutrients and to Particulate Organic Material: Fisheries Research Board of Canada Report 125, 192 p.

Thompson, R.S., 1992, Late Quaternary environments in Ruby Valley, Nevada: Quaternary Research, v. 37, p. 1–15, https://doi.org/10.1016/0033-5894(92)90002-Z.

Tingstad, A.H., Moser, K.A., MacDonald, G.M., and Munroe, J.S., 2011, A ~13,000-year paleolimnological record from the Uinta Mountains, Utah, inferred from diatoms and loss-on-ignition analysis: Quaternary International, v. 235, p. 48–56, https://doi.org/10.1016/j.quaint.2010.11.023.

Wagner, J.D.M., Cole, J.E., Beck, J.W., Patchett, P.J., Henderson, G.M., and Barnett, H.R., 2010, Moisture variability in the southwestern United States linked to abrupt glacial climate change: Nature Geoscience, v. 3, p. 110–113, https://doi.org/10.1038/ngeo707.

Wahl, D., Starratt, S., Anderson, L., Kusler, J., Fuller, C., Addison, J., and Wan, E., 2015, Holocene environmental changes inferred from biological and sedimentological proxies in a high elevation Great Basin lake in the northern Ruby Mountains, Nevada, USA: Quaternary International, v. 387, p. 87–98, https://doi.org/10.1016/j.quaint.2015.03.026.

Wayne, W.J., 1984, Glacial chronology of the Ruby Mountains–East Humboldt Range, Nevada: Quaternary Research, v. 21, p. 286–303, https://doi.org/10.1016/0033-5894(84)90069-3.

Zdanowicz, C.M., Zielinski, G.A., and Germani, M.S., 1999, Mount Mazama eruption: Calendrical age verified and atmospheric impact assessed: Geology, v. 27, p. 621–624, https://doi.org/10.1130/0091-7613(1999)027<0621:MMECAV>2.3.CO;2.

Manuscript Accepted by the Society 15 November 2017

Printed in the USA